AD_____

Award Number: DAMD17-99-2-9043

TITLE: Drug Development and Conservation of Biodiversity in West and Central Africa: Performance of Neurochemical and Radio Receptor Assays of Plant Extracts Drug Discovery for the Central Nervous System

PRINCIPAL INVESTIGATOR: Simon Efange, Ph.D.
Deborah C. Mash, Ph.D.

CONTRACTING ORGANIZATION: University of Miami
Miami FL 33136

REPORT DATE: September 2004

TYPE OF REPORT: Final

PREPARED FOR: U.S. Army Medical Research and Materiel Command
Fort Detrick, Maryland 21702-5012

REPORT DOCUMENTATION PAGE

Form Approved
OMB No. 0704-0188

1. REPORT DATE *(DD-MM-YYYY)*	**2. REPORT TYPE**	**3. DATES COVERED** *(From - To)*
01-09-2004	Final	1 SEP 1999 - 31 AUG 2004

4. TITLE AND SUBTITLE
Drug Development and Conservation of Biodiversity in West and Central Africa: Performance of Neurochemical and Radio Receptor Assays of Plant Extracts Drug Discovery for the Central Nervous System

5a. CONTRACT NUMBER

5b. GRANT NUMBER
DAMD17-99-2-9043

5c. PROGRAM ELEMENT NUMBER

6. AUTHOR(S)
(Simon Efange, Ph.D.; Deborah C. Mash, Ph.D.

E-Mail: dmash@med.miami.edu

5d. PROJECT NUMBER

5e. TASK NUMBER

5f. WORK UNIT NUMBER

7. PERFORMING ORGANIZATION NAME(S) AND ADDRESS(ES)
University of Miami
Miami FL 33136

8. PERFORMING ORGANIZATION REPORT NUMBER

9. SPONSORING / MONITORING AGENCY NAME(S) AND ADDRESS(ES)
U.S. Army Medical Research and Materiel Command
Fort Detrick, Maryland 21702-5012

10. SPONSOR/MONITOR'S ACRONYM(S)

11. SPONSOR/MONITOR'S REPORT NUMBER(S)

12. DISTRIBUTION / AVAILABILITY STATEMENT
Approved for Public Release; Distribution Unlimited

13. SUPPLEMENTARY NOTES

14. ABSTRACT
The thrust of the CNS assay panel was to identify plant extracts that display moderate to high affinity for selected molecular targets. Target selection was based identifying active plant extracts that would be useful for one or more neuropsyschiatric disorders. We completed a screen for 102 samples belonging to 43 plants. 41 showed activity at one or more CNS targets. Phytochemical studies have been initiated on several active extracts. A total of 12 plants samples which have tested positive for antiplasmodial activity were collected in bulk quantities for detailed phytochemical investigations into antimalarial and trypanocidal activity.

15. SUBJECT TERMS
CNS targets, drug discovery, phytochemistry

16. SECURITY CLASSIFICATION OF:			**17. LIMITATION OF ABSTRACT**	**18. NUMBER OF PAGES**	**19a. NAME OF RESPONSIBLE PERSON**
a. REPORT	**b. ABSTRACT**	**c. THIS PAGE**			USAMRMC
U	U	U	UU	34	**19b. TELEPHONE NUMBER** *(include area code)*

Table of Contents

Page

Introduction……1

Body……2-4

Key Research Accomplishments……4-6

Reportable Outcomes…… 7-9

Conclusion…… 10-12

References……13-14

Appendices…… 15-32

Drug Development and Conservation of Biodiversity in West and Central Africa: Performance of Neurochemical and radio receptor assays of plant extracts

Schuster, Brian George
Onugu, Tony

Final Report

Subcontract
Drug Discovery for the Central Nervous System
(Simon Efange, Ph.D., Principal Investigator; Deborah C. Mash, Ph.D., Miller School of Medicine,Contractor/Co-investigator).

Introduction

The thrust of the CNS assay panel was to identify plant extracts that display moderate to high affinity for selected molecular targets. The studies were conducted at the University of Miami School of Medicine under the supervision of Dr. Deborah C. Mash. Target selection was based identifying active plant extracts that would be useful for one or more neuropsyschiatric disorders. Extracts were assayed for binding to the following targets: dopamine and serotonin transporters, dopamine D3 receptors, mu and kappa opioid receptors, and [^{3}H]epibatidine binding sites (nicotinic acetylcholine receptors). Plant extracts were initially subjected to a two-point assay (0.8 and 80 ug/ml) and those displaying greater than 50% inhibition of radioligand binding at a concentration of 80 mg/ml were chosen for IC50 determination. Extracts displaying IC50 values less than 50 ug/ml (which value corresponds to an IC50 of about 600 nM for a compound which comprises 0.5% of the mixture and has a molecular weight of 400 g/mol) were selected for detailed phytochemical study aimed at identifying the active ingredient(s). Extracts displaying IC50s between 50 and 300 ug/ml were fractionated into four major fractions. Fractions which displayed IC50 values lower than 50 ug/ml were also selected for study.

Body

1.] The main objective of these studies was to identify the CNS activity of ethnobotanical plant extracts and some identified fractions using specific radioligand binding assays.

2.] These assays were designed to identify activity at particular CNS receptor or transporter sites and to determine whether the extract contained a full or partial agonist or antagonist.

The development of novel CNS medications for neuropsychiatric disorders is based on the premise that the simultaneous modulation of two or more neural mechanisms (multiple-target agents) provides a more effective approach for treatment than current single-target approaches. Plants used by indigenous cultures for traditional initiation rites and/or for the treatment of neuropsychiatric disorders may provide suitable leads for developing novel CNS pharmacotherapies. This hypothesis is based on the recognition that such plants often contain neuroactive ingredients which may be used as lead compounds for modulating central serotonin and dopaminergic function, two neurochemical systems that are implicated in major psychiatric disorders. Such plants may also reveal novel mechanisms for the management of these disease states.

Revolutionary advances in basic preclinical and clinical Neuroscience have catalyzed unprecedented efforts toward the discovery and development of novel CNS drugs which should prove effective for the treatment of neuropsychiatric disease. These advances have included the molecular cloning and characterization of many of the neurochemical mediators (Kilty et al, 1991; Vandenbergh et al.,1992; Giros et al, 1992; Sibley and Monsa, 1992). The specificity of neurotransmitter-related signaling lies both in the anatomic distribution of a given neurotransmitter, as well as in the distribution and heterogeneity of the receptors (and related proteins) recognized by these neurotransmitters. Current drug discovery efforts have taken advantage of this heterogeneity. The receptor binding assay is one of the most important analytical tools and methodologies that have revolutionized Neuroscience research. The development of binding assays for drugs, hormones and neurotransmitters has provided specific and rapid methods for identifying sites associated with the molecule that functions either to activate or inhibit a receptor-mediated neural signaling.

The rationale for our drug discovery research focusing on novel plant-based medicines was based on the recognition that plants are an important source of lead compounds for novel CNS active drugs. Modern medicine traces its origins to Man's use of plant and animal parts in alleviating human suffering caused by disease. Some of the earliest compilations of the medicinal uses of plants include the *De materia medica* of Dioscorides (78 A.D.) and the Egyptian *Papyrus Ebers* (1550 B.C). A review of the literature shows that prior to 1970, there was a strong interest in examining plants as sources of new pharmaceutical agents. According to Fansworth et al. (1985), over 120 pharmaceutical products in use as of 1985 were derived from plants. Of these agents, more than seventy per cent were discovered by examining the use of these plants in traditional settings by examining there ethnomecial use practices. The commercial production of these agents is largely by extraction of active compounds from about 90 plant species. On the this basis, it has been suggested that plants remain an important source of new drugs (Farnsworth, 1994).

Modern and new advances in synthetic and computational chemistry, molecular neurobiology and genetic engineering produced a decline in emphasis on plant-derived leads especially for CNS drugs. It was forecast not so many years ago that single drug substances resulting from rational design and synthesis would replace the old fashioned herbal plants which had been the mainstay of medicial treatment for many centuries. Today there is an increasing awareness of the loss of biological diversity resulting from rapid deforestation of the tropical regions of the world, coupled with a realization of the enormous chemical diversity of the plant kingdom which remains unexplored and in danger of extinction. This change in drug discovery stems from the advent of anticancer agents paclitaxel (Taxol), discodermolide and epothilone A & B. Multimillion-dollar efforts have been directed to undertake a highly focused search for new drugs from ethnomedical leads. In 1997 the National Institutes of Health, through the Fogarty International Center (FIC), instituted an experimental program, the International Cooperative Biodiversity Groups (ICBG) Program, that addresses the interdependent issues of drug discovery, biodiversity conservation and sustainable economic growth (C&EN, April 7, 1997).

The search for new ethnobotanical drugs stem from the random collection and mass screening of plant extracts. (Adjanohoun et al., 1996, Bever, 1986 Iwu et al., 1999) The advantage of the ethnomedicine approach is that when properly executed, it takes into account the accumulated knowledge base of cultural plant use, thereby increasing the probability that novel compounds with known indications for use will be discovered. (Harbone, 1998, Iwu, 1993. Tabuti et al., 2003) Our project was based on the hypothesis that plants used by indigenous cultures for traditional medicine and/or for the treatment of neuropsychiatric disorders might provide suitable leads for developing novel therapies. This hypothesis was based on the recognition that such plants often contain neuroactive ingredients which may be used as lead compounds for modulating central dopaminergic, serotonergic and opiatergic function. Such plants might also reveal novel compunds for the management of endemic tropical diseases such as malaraia, trypanonosomiasis, and chronic bacterial pathogens (Fabry et al., 1996, Tchuendem et al., 1999. Ogbeche et al., 1997).

Research Accomplishments

Over the project period a total of 102 samples each assaysed in twice were processed for binding site activities. The extracts were provided as blinded samples with accession numbers to the ICBG work group. Estimated crude weights were provided as shown in table 1.

Table 1: ICBG PLANT SAMPLES

In House Sample#	SU-Lab Number	Plant Part	Wt given (mg)
ICBG 1	SU1904	Whole Plnt	25
ICBG 2	SU1905	Sd Pulp	25
ICBG 3	SU1906	Pn polar	25
ICBG 4	SU1907	Lf/Stem	25
ICBG 5	SU1908	Lf/stem	25
ICBG 6	SU1909	Stbk	25
ICBG 7	SU1910	Stbk	25
ICBG 8	SU1911	Stbk	25
ICBG 9	SU1912	Whole Plnt	25
ICBG 10	SU1913	Whole Plnt	25
ICBG 11	SU1914	Ft pulp	25

Methods

Preparation of Extracts: Stocks of the solid extracts were prepared by weighing 4 mg of sample and diluting to a total volume of 5 ml with 50% ethanol solvent for a final concentration of 0.8 mg/ml.

Ligand Binding Assays. Brain tissues were homogenized with a Brinkmann polytron for 15 secs (setting of 3) in the appropriate assay buffer. After 30 min on ice, membranes were collected by centrifugation for 10 minutes at 30,000 x g and resuspended in assay buffer. For binding assays, membranes from tissues (0.5 to 10 mg/ml) were incubated in assay buffer with the radioligand and 10 μM concentrations of test compound for each assay. Competition assays were performed with at least 6 concentrations. The test compound, including total, reference compound and nonspecific tubes were included with each assay run. Competition assays were run in duplicate. All incubations were terminated by vacuum filtration over Whatman 934AH glass fiber filters presoaked in polyethyleneimine. Filters were washed two to three times with ice-cold binding buffer, and counted for radioactivity in 4 ml Cytoscint (Isolab, Irvine, CA) at an efficiency of 50%.

To prepare cloned cell membranes, medium is removed and cells are washed with calcium and magnesium free PBS buffer. Cells are allowed to sit for at least 10 min, scraped and pelleted by centrifugation. The cell membrane pellet is re-suspended in assay buffer in an appropriate concentration of protein prior to assay. Ligand binding assays are conducted as for membranes prepared from brain tissues as described below.

5-HT Transporter.. Labeling of the 5-HT transporter was carried out as described previously (Staley et al., 1994). Briefly, occipital cortex tissue samples were homogenized in ice-cold 10 mM $NaPO_4$, pH 7.4, 0.32 M sucrose. Membranes were pelleted by centrifugation at 30,000 x g for 10 min at 4 ^{o}C and washed once in a similar manner. Competition assays were conducted with membrane homogenates (2.5 mg/ml, original wet weight/ml) and [^{125}I]RTI-55 (10 pM) in the presence of 1 uM benztropine in a final volume of 2 mls for 1 h at 25^{o}C. Nonspecific binding was determined with 50 uM (-) cocaine.

DA transporter. The DA transporter is a primary target for the reinforcing effects of drugs and for CNS disorders such a schizophrenia. The potency for binding to the DA transporter were determined using [^{3}H]WIN 35,428 as described previously (Mash et al 2002). Briefly, membrane homogenates from the human caudate were prepared as described for the 5-HT transporter. Binding assays were conducted in assay tubes containing a total volume of 2 ml, 10 pM [^{3}H]WIN 35,428, and 1 mg of caudate membranes. Nonspecific binding were defined in the presence of 50 μM (-) cocaine. Total radioligand bound were separated from free radioligand by rapid filtration after a 1 h incubation at 25^{o}C as described for the 5-HT transporter.

Opioid Receptor(Mμ) Ligand Binding: Two-point binding screens using [^{3}H]DAMGO were performed as per methods described within the grant and previously (Rothman et al., 1995). Briefly, monkey thalamus was homogenized in ice-cold buffer (1:10 w/w, 50 mM Tris, 5 mM $MgCl_2$, pH 7.6), centrifuged at 32,000 x g for 20 min, and the supernatant was discarded. The pellet was washed with same and centrifuged again. The pellet was resuspended (1:10, w/w) with buffer, and 100 ml was added to each tube for a final concentration of 10.0 mg/ml (original tissue wet weight), in a final assay tube volume of 1.0 ml. Screens were performed by incubating 2 concentrations of extract (0.8 and 80 mg/tube) in the presence 1.0 nM of radioligand for 2 hr at 25°C, to determine their inhibitory potency (% inhibition). Nonspecific binding was determined by binding in the presence of 10 mM naloxone. Incubations were terminated by vacuum filtration through glass fiber filters (Whatman 934-AH) presoaked in 0.1% polyethylenimine (PEI) followed by washing with ice-cold buffer (3 x 4 ml).

Data Analysis: Data are analyzed using the non-linear regression algorithms found in EBDA/LIGAND™ and GraphPad Prism™ computer software programs.

Reportable Outcomes

Table 2: Plant Extract Activity (% inhibition) on DAT, SERT & Mμ

	DAT ([^{3}H]WIN35,428)		*SERT*([^{125}I]RTI-55)		*Mμ*([^{3}H]DAMGO)	
In House Sample#	@ 0.8 mg/tube	@ 80 mg/tube	@ 0.8 mg/tube	@ 80 mg/tube	@ 0.8 mg/tube	@ 80 mg/tube
ICBG 1	--	58.7		42.0	1.8	60.4
ICBG 2	--	46.3	--	90.1	16.7	60.2
ICBG 3	--	18.8	--	46.7	31.8	39.4
ICBG 4	--	77.7	--	--	33.0	41.0
ICBG 5	--	22.9	--	--	--	33.3
ICBG 6	--	27.2	--	20.5	--	33.4
ICBG 7	--	--	--	--	--	29.6
ICBG 8	--	50.6	--	31.0	10.3	29.2
ICBG 9	--	82.0	--	--	--	32.8
ICBG 10	--	74.9	3.9	76.1	28.6	32.9
ICBG 11	--	--	--	87.2	32.4	47.1

-- denotes no inhibitory activity

As can be seen in Table 2, a number of extracts inhibited greater than 50% of the binding at DAT, SERT and mu opiate receptors. Functional assays were done based on the availability of purified fractions to isolate bioactive compounds for further characterization.

Results: We completed a screen for 102 samples belonging to 43 plants. At this time, fifty percent of them have been screened in 3 assays (mu-opioid, dopamine D3 and [^{3}H]nicotine) while the others have been tested in six assays (mu-opioid, kappa-opioid, dopamine D3, DAT, SERT and [^{3}H]nicotine). Preliminary and confirmatory screening has identified 25 plant extracts for further investigation (see Table 3). Several extracts have undergone confirmatory screening to determine IC50 values. A number of extracts such as those from *Jatropha curcas, Emilia coccinea, Justicia insularis, Solanum aculeastrum and Stephania* appear to be active at the mu opioid receptor. So far, only four extracts show any activity at nicotinic receptors. The most active extract from *Pericopsis laxifolia* serves as an internal control since the latter is known to contain the potent nicotinic agonist cytisine. An interesting finding relative to *P. laxifolia* is the rather significant level of activity at mu opioid receptors, and the modest level of activity at dopamine D3 receptors. So far, we can find no mention of cytisine acting as a mu agonist or antagonist. Consequently, further investigation of this finding may yield some interesting

possibilities. Among the possibilities for the dopamine D3 receptor are *Stephania abyssinica, Clematis hirsuta, Laportea aestuans, Pericopsis laxifolia* and *Jatropha curcas.* Finally, although *Rauwolfia vomitaria* is well known for its effects on monoaminergic systems, it would appear our recent studies have identified a constituent with activates mu opioid receptors. The presence of mu opioid agonists and antagonists has been documented for *Picralima nitida,* a related apocynaceous plant (Menzies et al., 1998; Arens et al., 1982; vide infra). Our results are thus in agreement with these earlier observations. A more intriguing finding is the pronounced activity at nicotinic receptors. With confirmation, this avenue of investigation may yet expose another side to an otherwise interesting plant.

Plants collected for the CNS investigation were also tested for antiplasmodial activity. So far, four of them namely *Aneilema umbrosum, Eriosema glomerata, Pittosporum viridiflorum and Scleria spp,* have displayed significant antiplasmodial activity and been selected for further study.] The screening exercise thus has the potential to yield dividends in all segments of drug discovery that are of interest to this project. Phytochemical studies had been launched to identify the active priniciples of a number of the neuroactive and antimalarial plants. These studies were not continued due to a lack of continuation support for the project.

Table 3. Plant Extracts Showing Activity at Selected CNS Targets.

NAME OF PLANT (part used)	SU #	SOLVENT	% INHIBITION AT 0.8/80 ug/ml or IC50 (ug/ml, BOLD)					
			DAT	SERT	Mu Opioid	Kappa-1 Opioid	Nicotine	Dopamine D3
Ancistrocladus barteri	SU1911		**80**			---/64		
C. filiformis (whole plant)	SU1904	MeOH						
Dracaena mannii (fruit pulp)	SU 1914	MeOH		**7**	32/47			
Erythrophleum guineensis	1909	MeOH			--/38	--/52		
P. nitida	SU1905	MeOH	--/50	**4**				
Scoparia dulcis (whole plant)	SU1912	MeOH	**10**			--/64	**182**	
Scoparia dulcis	SU 1913	CH_2Cl_2	**12**	**11**		--/74		
Triumfetta tomentosa	SU							
Aneilema umbrosum (whole plant)	SU2302	CH_2Cl_2	10/45		--/77			
Aneilema umbrosum (whole plant)	SU2303	MeOH	10/47		6/54			
Cissus quandrangularis (whole plant)	SU2360	CH_2Cl_2			**94**			
Cissus quandrangularis (whole plant)	SU2361	MeOH			**138**			
Clematis hirsuta (aerial parts)	SU2340	CH_2Cl_2	--/65		**54**			**145**
Clematis hirsuta (aerial parts)	SU2341	MeOH	29/32		**124**			
Crinum purpurascens (bulb)	SU2288	CH_2Cl_2	--/57		**90**			**2354**
Dichrocephala integrifolia (whole plant)	SU2292	CH_2Cl_2			**98**			
Emilia coccinea	SU2579	CH_2Cl_2			**38**			
Eriosema glomerata (aerial parts)	SU2324	CH_2Cl_2			**211**			
Jatropha curcas (aerial parts)	SU2379	MeOH	37/44		**41**			**261**
Justicia insularis (whole plant)	SU2282	CH_2Cl_2			**85**		18/30	
Justicia insularis (whole plant)	SU2283	MeOH			**91**		**194**	
Kalanchoe crenata (whole plant)	SU2306	CH_2Cl_2			**101**			
Laportea aestuans (whole plant)	SU2354	CH_2Cl_2	9/35		6/57			
Laportea aestuans (whole plant)	SU2355				-/31			
Maytenus senegalensis (leaves)	SU2580	CH_2Cl_2						**292**
Mucuna pruriens (leaves)	SU2637	CH_2Cl_2			**542**			
Mucuna pruriens (leaves)	SU2638	MeOH			**88**			
Pentaclethra macrophylla (fruit bark)	SU2589	CH_2Cl_2			**606**			
Pericopsis laxifolia (leaves)	SU2643	CH_2Cl_2			**53**		**55**	**285**
Pittosporum viridiflorum (stem bark)	SU2336	CH_2Cl_2	--/61		**186**			
Pittosporum viridiflorum (stem bark)	SU2337	MeOH	--/61		**585**			
Pterocarpus soyauxii (stem bark)	SU2384	CH_2Cl_2	--/42					
Rauwolfia vomitaria (stem bark)	SU2520	CH_2Cl_2	--/85	16/99	14/89		--/88	
Rauwolfia vomitaria (stem bark)	SU2522	MeOH	26/96	88/96	71/91		49/100	
Solanum aculeastrum (leaves)	SU2350	CH2Cl2			**28**			
Spilanthes africana (whole plant)	SU2296	CH2Cl2			**98**			
Stephania abyssinica (aerial parts)	SU2587	CH2Cl2			**57**			**131**
Stephania abyssinica (aerial parts)	SU2588	MeOH			**69**			**74**
Synsepalum longecuneatum (bark)	SU2344	CH2Cl2			**203**			
Trema occidentalis (stem bark)	SU2650	CH2Cl2			**236**			
Trema occidentalis (stem bark)	SU2650	MeOH			**441**			

Conclusions

Phytochemical Studies.

CNS disorders: Phytochemical studies have been initiated on several active extracts. For the CNS component, phytochemical studies have been initiated on *Cassytha filiformis, Mitragyna stipulosa, Dracaena mannii, Triumfetta tomentosa, Baillonella toxisperma, Peucedanum zenkeri, Scoparia dulcis and Cissus quandrangularis.* Studies of *P. zenkeri* were initiated because this plant is used by cattle herders in parts of Cameroon as a tobacco substitute. Pharmacological screening of a seed extract of this plant revealed significant antiparasitic activity. Thee results of this studies are discussed below under antiparasitic activity. So far, more than 30 metabolites have been isolated from the plants listed above; these will be characterized by proton and C-13 NMR and mass spectrometry, and subjected to pharmacological evaluation.

Malaria & Trypanonosomiasis

A total of 12 plants samples, including Odyendyea gabunensis, which has tested positive for antiplasmodial activity were collected in bulk quantities for detailed phytochemical investigations. Extracts and pure compounds from three plants including *Khaya senegalensis, anthocleista vogelii, and Miletia spp* were forwarded to Dr Bacchi for anti-trypanosomal and and anti-fungal bioassays. The stem bark and leaves of Odyendyea gabunensis were extracted with a mixture of methylene chloride/methanol (1/1) and the extracts subjected to chromatographic separation leading to the isolation of 12 pure secondary metabolites. The structural elucidation and biological evaluation of these samples is currently under way.

Training

University of Dschang: A total of five graduate thesis/dissertations were submitted and successfully defended in 2002 by students working on project. These include one Doctorat 3e Cycle", three Mphil and two Msc degrees awarded under the direction of Dr. Simon Efange or collaborators. On July 2002, two students, Mr. Pierre Celestin Djemgou and Mrs Roukayatou Mbouangouere presented their theses and were awarded the M.Phil. degree. The third M.Phil thesis was defended on November by Simplice Tatsimo. All of them are now enrolled in the Ph.D programme at the Univsersity of Dschang. Finally, in November, Valatine Alang Mail and Eric W. Pefoute were awarded M.Sc degrees and are enrolled in M.Phil program.

University of Buea: Four students were enrolled in the M.Sc. program. They were expected to graduate by the latter half of 2003.

Publications

DD. DeCarvalho, A. C. V., Ndi, C. P., Tsopmo, A., Tane, P., Ayafor, J., Connolly, J. D. and Teem, J. L. (2002) A Novel Natural Product Compound Enhances cAMP-Regulated Chloride Conductance of CellsExpressing CFTRDF508. *Molecular Medicine,* 8, 75-87.
APPENDIX

Kamnaing P, Tsopmo A, Tanifum EA, Tchuendem MH, Tane P, Ayafor JF, Sterner O, Rattendi D, Iwu MM, Schuster B, Bacchi C. Trypanocidal diarylheptanoids from Aframomum letestuianum. J Nat Prod. 2003 Mar;66(3):364-7.
APPENDIX

Ngwendson JN, Bedir E, Efange SM, Okunji CO, Iwu MM, Schuster BG, Khan IA. Constituents of Peucedanum zenkeri seeds and their antimicrobial effects. Pharmazie. 2003 Aug;58(8):587-9.

References

J.F. Adjanohoun, N. Aboubakar, K. Dramane, M.E. Ebot, J.A. Ekpere, E.G. Enow-Orock, D. Focho, Z.O. Gbile, A. Kamanyi, J. Kamsu Kom, A. Keita, T. Mbenkum, C.N. Mbi, B. Nkongmeneck, B. Satabie, A. Sofowora, V. Tamze and C.K. Wirmum, Traditional Medicine and Pharmacopoeia: Contribution to Ethnobotanical and Floristic Studies in Cameroon, Organization of African Unity, Scientific, Technical and Research Commision. Centre Nationale de Production des Manuels Scolaires, Porto-Novo, Benin (1996) pp. 207–209.

B.O. Bever, Medicinal plants of tropical West Africa, *Anti-infective Activity of Chemical Components of Higher Plants*, Cambridge University Press, Cambridge (1986) pp. 68–70.

W. Fabry, P. Okemo and R. Ansorg, Activity of East African medicinal plants against *Helicobacter pylori*, *Chemotherapy* **42** (1996), pp. 315–317.

N.R. Farnsworth, Akerele O, Bingel AS, Soejarto DD, Guo Z. Medicinal plants in therapy. Bull World Health Organ. 1985;63(6):965-81.

N. R. Farnsworth. Ethnopharmacology and drug development.Ciba Found Symp. 1994;185:42-51; discussion 51-

B. Giros,, El-Mestikawy, S., Godinot, N., Zheng, K., Han, H., Yang-Feng, T., Caron, M.G. (1992b) Cloning, pharmacological characterization and chromosome assignment of the Human Dopamine Transporter. Molec. Pharmacol. 42:383-390.

J. B. Harbone, Phytochemical methods, *A Guide to Modern Techniques of Plant Analysis* (3rd ed.), Chapman and Hall, London (1998) pp. 23–30.

M.W. Iwu, A.R. Duncan and C.O. Okunji, New antimicrobials of plant origin. In: J. Janick, Editor, *Perspectives on New Crops and New Uses*, ASHS Press, Alexandria, VA (1999), pp. 457–462.

M.M. Iwu , Handbook of African Medicinal Plants. , CRC Press, London

(1993).

J.E. Kilty, Lorang, D., Amara, S.G. (1991) Cloning and expression of a cocaine-sensitive rat dopamine transporter. Science 254:578-579.

D. C. Mash, Pablo J, Ouyang Q, Hearn WL, Izenwasser S. Dopamine transport function is elevated in cocaine users. J Neurochem. 2002 Apr;81(2):292-300.

A.K. Ogbeche, G.O. Ajayi and P. Onyeneta, Antibacterial activities of the leaf extract of *Ageratum conyzoides*, *Nigerian Quarterly Journal of Hospital Medicine* **7** (1997), pp. 397–399.

D. R. Sibley, , Monsa, F.J., Jr. (1992) Molecular biology of dopamine receptors. TIPS 13:61-69.

J. K. Staley, Basile, M., Flynn, D.D., Mash, D.C. (1994) Visualizing dopamine and serotonin transporters in the human brain with the potent cocaine analogue [^{125}I]RTI-55: In vitro binding and autoradiographic characterization. J. Neurochem. 62:549-556

J.R.S. Tabuti, S.S. Dhillion and K.A. Lye, Traditional medicines in Bulamogi County, Uganda: its practitioners, users and viability, *Journal of Ethnopharmacology* **85** (2003), pp. 119–129.

M.-H.K. Tchuendem, J.A. Mbah, A. Tsopmo, J.F. Ayafor, O. Sterner, C.C. Okunji, M.M. Iwu and B.M. Schuster , Antiplasmodial sesquiterpenoids from the African *Reneilmia cincinnata*. *Phytochemistry* **52** (1999), pp. 1095–1099.

D. J. Vandenbergh, Persico, A.M., Uhl, G.R. (1992) A human dopamine transporter cDNA predicts reduced glycosylation, displays a novel repetitive element and provides racially-dimorphic TaqI RFLPs. Molec. Brain Res. 15(1-2):161-166.

Molecular Medicine 8(2): 75–87, 2002

A Novel Natural Product Compound Enhances cAMP-Regulated Chloride Conductance of Cells Expressing CFTRΔF508

Ana C. V. deCarvalho,[1] Chi P. Ndi,[2] Apollinaire Tsopmo,[2] Pierre Tane,[2] Johnson Ayafor,[2] Joseph D. Connolly,[3] and John L. Teem[1]

[1]Department of Biological Science, Florida State University, Tallahassee, FL, USA

[2]Department of Chemistry, Faculty of Science, University of Dschang, Dschang, Cameroon

[3]Department of Chemistry, University of Glasgow, Glasgow, UK

Accepted January 25, 2002

Abstract

Background: Cystic fibrosis (CF) results from mutations in the cystic fibrosis transmembrane conductance regulator (CFTR) gene, which encodes a chloride channel localized at the plasma membrane of diverse epithelia. The most common mutation leading to CF, ΔF508, occurs in the first nucleotide-binding domain (NBD1) of CFTR. The ΔF508 mutation disrupts protein processing, leading to a decreased level of mutant channels at the plasma membrane and reduced transepithelial chloride permeability. Partial correction of the ΔF508 molecular defect in vitro is achieved by incubation of cells with several classes of chemical chaperones, indicating that further investigation of novel small molecules is warranted as a means for producing new therapies for CF.

Materials and Methods: The yeast two-hybrid assay was used to study the effect of CF-causing mutations on the ability of NBD1 to self-associate and form dimers. A yeast strain demonstrating defective growth as a result of impaired NBD1 dimerization due to ΔF508 was used as a drug discovery bioassay for the identification of plant natural product compounds restoring mutant NBD1 interaction. Active compounds were purified and the chemical structures determined. The purified compounds were tested in epithelial cells expressing CFTRΔF508 and the resulting effect on transepithelial chloride permeability was assessed using short-circuit chloride current measurements.

Results: Wild-type NBD1 of CFTR forms homodimers in a yeast two-hybrid assay. CF-causing mutations within NBD1 that result in defective processing of CFTR (ΔF508, ΔI507, and S549R) disrupted NBD1 interaction in yeast. In contrast, a CF-causing mutation that does not impair CFTR processing (G551D) had no effect on NBD1 dimerization. Using the yeast-based assay, we identified a novel limonoid compound (TS3) that corrected the ΔF508 NBD1 dimerization defect in yeast and also increased the chloride permeability of Fisher Rat Thyroid (FRT) cells stably expressing CFTRΔF508.

Conclusion: The establishment of a phenotype for the ΔF508 mutation in the yeast two-hybrid system yielded a simple assay for the identification of small molecules that interact with the mutant NBD1 and restore dimerization. The natural product compound identified using the system (TS3) was found to increase chloride conductance in epithelial cells to an extent comparable to genistein, a known CFTR activator. The yeast system will thus be useful for further identification of compounds with potential for CF drug therapy.

Introduction

Cystic fibrosis (CF) is a lethal human genetic disease resulting from mutations in the cystic fibrosis transmembrane conductance regulator (CFTR) gene (1–3). The protein encoded by the CFTR gene is a cAMP-regulated chloride channel located in the apical membrane of epithelial cells in various tissues (4). CFTR is a member of the ABC transporter superfamily of proteins that are involved in translocation of a diverse set of substrates across biological membranes in both prokaryotes and eukaryotes (5). It has been proposed that a functional ABC transporter has a minimal structural requirement of two membrane-spanning domains (MSDs) and two cytosolic nucleotide binding domains (NBDs) that can be present in a single polypeptide or formed by a membrane-associated multiprotein complex (6).

The most common mutation causing CF is the in-frame deletion of a phenylalanine at position 508 (ΔF508) in the first nucleotide binding domain of CFTR (NBD1), occurring in ~70% of CF chromosomes. The ΔF508 mutation impairs processing of CFTR in the endoplasmic reticulum (ER), resulting in decreased levels of mature CFTR at the plasma membrane and defective cAMP-regulated chloride conductance in diverse epithelia. A large fraction of CFTRΔF508 fails to fold into a native conformation, resulting in its retention by the ER-associated quality control and subsequent degradation with the participation of the cytoplasmic proteasome (7–11). In addition to the biosynthetic defect, the ΔF508 mutation also affects the chloride channel function of CFTR, reducing the channel open probability (P_o)

Address correspondence and reprint requests to: John Teem, Department of Biological Science, Biounit-238, Florida State University, Tallahassee, Florida 32306, USA. Phone: (850) 644-5121; fax: (850) 644-0481; e-mail: teem@bio.fsu.edu

(12–14). Partial reversal of the processing defect resulting from ΔF508 can be achieved by altering conditions in which cultured cells expressing the mutant CFTR are incubated. For example, addition of glycerol in high concentration to the culture media (15,16) or reduction of the cell culture incubation temperature (17) partially restore CFTRΔF508 processing. Additionally, several CFTR activators have been developed that can enhance activity of the mutant chloride channel at the plasma membrane (18,19).

The ΔF508 mutation is thought to affect the folding of the NBD1 domain polypeptide (20,21), leading to defective processing and function of the mutant CFTRΔF508 protein. The precise effect of ΔF508 on NBD1 structure is unknown because a crystal structure of CFTR NBD1 is currently unavailable. Dimerization of NBDs has been observed for the subunits of bacterial ABC transporters HisP and MalK (22–25), and for the ER and peroxisomal localized ABC transporters (26). Thus, dimerization of CFTR NBDs may similarly occur, and the ΔF508 mutation may interfere with NBD1 folding such that dimerization is defective.

Using the yeast two-hybrid system, we have established that CFTR NBD1 is able to interact with itself in vivo, and that the ΔF508 mutation impairs this interaction. We have used the yeast two-hybrid assay in a drug screening format to identify a novel limonoid compound that reverses the ΔF508 dimerization defect in yeast and promotes increased cAMP-stimulated chloride current from mammalian cells expressing CFTRΔF508. The identification of compounds that specifically target and rescue CFTRΔF508 could lead to the development of a therapy for CF.

Materials and Methods

Plasmid Construction and Yeast Strains

The plasmid pSwick-CFTR containing the full-length wild-type CFTR cDNA was obtained from M. Welsh (University of Iowa) and amplified by the polymerase chain reaction (PCR) with the appropriate oligonucleotide primers to generate a DNA segment corresponding to CFTR NBD1 and upstream linker region, T351-F650. The T351-F650 segment was cloned in-frame into the carboxy-terminus of the GAL4 DNA-binding domain on a yeast plasmid pBDGAL4 (Stratagene Cloning Systems, La Jolla, CA, USA). The resulting plasmid (pBDNBD1) contains a fusion protein consisting of the GAL4 DNA binding domain fused to CFTR NBD1 (T351-F650) expressed under the control of the yeast ADH1 promoter and also contains the yeast selectable marker TRP1 and the 2μ origin of replication. The same segment of CFTR NBD1 was also cloned in-frame into the GAL 4 activation domain on pADGAL4 (with the yeast selectable marker LEU2 and 2μ origin) to produce pADNBD1. Both plasmids pBDNBD1 and pADNBD1 were introduced by transformation into yeast strain YGR-2 (HybriZap Two Hybrid Cloning Kit, Stratagene), genotype: *Matα, ura3-52, his3-200, ade2-101, lys2-801, trpl-901, leu2-3, 112, gal4-542, gal80-538,* LYS2::UAS_{GAL1}-$TATA_{GAL1}$-HIS3 URA::$UAS_{GAL4\ 17mers(x3)}$ $TATA_{CYC1}$-lacZ) and transformants were selected on selective media lacking tryptophan and leucine to produce the yeast strain YRG2-WT. Plasmids identical to pBDNBD1 and pADNBD1, but containing CF-causing mutations (ΔF508, ΔI507, S549R, and G551D) were similarly constructed (producing pBDΔF, pADΔF, pBDΔI507, pADΔI507, pBDS549R, pADS549R, pBDG551D, pADG551D). Plasmids pBDΔF and pADΔF were introduced by transformation into yeast strain YGR-2 to produce yeast strain YRG2-ΔF. Other yeast strains expressing GAL4/CFTR NBD1 fusion proteins containing CF-causing mutations were constructed by transformation with the cognate pBDNBD1 and pADNBD1 derivatives. The YRG-2 control strain used in Figure 4 contained pBDGAL4 (lacking CFTR NBD1 sequences) and pADNBD1. The DNA structure of the constructs was confirmed by DNA sequence analysis.

pBDGAL4	pADGAL4
NBD1 WT	NBD1 WT
NBD1 Δ F508	NBD1 Δ F508
NBD1 Δ I507	NBD1 Δ I507
NBD1 S549R	NBD1 S549R
NBD1 G551D	NBD1 G551D
P53	NBD1 WT
NBD1 WT	T-antigen

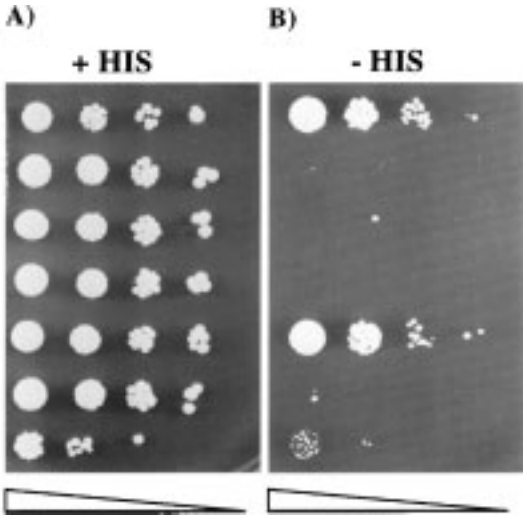

Fig. 1. Effect of CF mutations on NBD1 interaction in the yeast two-hybrid system. The yeast strain YRG-2 was cotransformed with the pBDNBD1 and pADNBD1 plasmids as indicated. pADNBD1 and pBDNBD1 were co-expressed with pBDGal4 p53 and pADGal4 T-antigen, respectively, as controls. Equal aliquots of serial dilutions of each yeast strain were plated on –Leu –Trp medium **(A)** and on –Leu –Trp –His selective medium containing 5 mM AT **(B)**. Triangles indicate increasing dilution of each culture. Plates were incubated for 3 days at 30°C.

Yeast Two-Hybrid Assay

YRG-2 yeast strains expressing the pADNBD1 and pBDNBD1 variants were plated on selective medium lacking histidine as described by the supplier (Stratagene), supplemented with 1.5–5 mM 3-amino-1,2,4-triazole (AT) and incubated at 30°C for 3 days.

Bioassay-Directed Fractionation

Leaves of *Trichilia* sp. c.f. *rubescens* Oliv. were collected from Korup reserve, South West Province of Cameroon. Air-dried powdered leaves (2.7 kg) were macerated in acetone (8 l) at room temperature for 3 × 2 days. Filtration and vacuum concentration led to a dark greenish extract (154 g). This extract was dissolved in a mixture of H_2O-MeOH (9:1) and subsequently extracted with hexane and CH_2Cl_2 to afford 47.5 g and 42.5 g of the hexane-soluble fraction and CH_2Cl_2-soluble fraction, respectively. Vacuum liquid chromatography on SiO_2 of the CH_2Cl_2 extract (which contained the bioactivity) eluted with gradients of EtOAc in hexane led to five main fractions (F1–F5) of increasing polarity. Only fractions F3 and F4 yielded positive results in the yeast two-hybrid bioassay. F3 (1.2 g) eluted with hexane-EtOAc (8:2) was then passed through a silica gel column using CH_2Cl_2 to give a mixture that was further purified on chromatotron using Me_2CO-CH_2Cl_2 (2:98) to give TS2 (80 mg) and a mixture of unresolved compounds. F4 (0.9 g), also eluted with hexane-EtOAc (8:2), was purified in the same way as fraction F3 to yield TS1 (40 mg) and TS3 (133 mg). An additional purification of TS1 and TS3 by gel permeation through Sephadex LH-20 (to remove chlorophyll) was required to obtain pure analytical samples.

Experimental Procedures for Structure Determination

Melting points were recorded with a kohfler hot stage 277938 and are uncorrected. Optical rotations were measured on an AA Series automatic polarimeter POLAAR-2000, while the IR spectra were recorded on a JASCO FT-IR–410 spectrophotometer. ^{1}H NMR (400 MHz) and ^{13}C NMR (100 MHz) spectra were recorded in $CDCl_3$ on BRUKER DPX–400 spectrometer. The chemical shifts (δ) are reported in parts per million (ppm) relative to chloroform signals as reference (δ_H = 7.26 and δ_C = 77.0) and coupling constants (J values) are given in Hertz. ^{1}H-^{1}H COSY, NOE's, HMBC, and HMQC experiments were recorded with gradient enhancements using sine-shaped gradient pulses. Mass spectra were recorded in the positive EI mode on a JEOL JMS–700 instrument. Column chromatography, run on Merck Si gel 60, and gel permeation chromatography on Sephadex LH-20 were used for isolation and purification. TLC were carried out on silica gel 60 F_{254} (Merck) precoated plates and spots visualized by spraying with 50% H_2SO_4 solution followed by heating, or with UV lamp (254 and 366 nm).

Spectroscopic Analysis of Limonoid Compounds

TS1 was obtained as white crystals in hexane, mp 292–294°C, $[\alpha]_D^{25}$ + 32.5° (*c* 0.6, $CHCl_3$). The EIMS of TS1 gave a molecular ion peak at *m/z* 438 compatible with molecular formula $C_{26}H_{30}O_6$. The TS1 IR spectrum showed peaks at υ_{max} 3437 and 1664 cm^{-1} attributed to hydroxyl group and enone moiety, respectively. The ^{1}H NMR spectrum for TS1 (Table 1) showed proton signals at δ7.36 (d, J = 1.6 Hz), 7.13 (s), and 6.18 (d, J = 1.6 Hz) which were attributed to a furan ring (27), while proton signals at δ5.93 (d, J = 9.5 Hz) and 7.08 (d, J = 9.5 Hz) were attributed to H-2 and H-3, respectively. Many other proton signals were observed including four methyl groups between δ1.41–0.80. The ^{13}C NMR spectrum (Table 2) showed the presence of a carbonyl group at δ200.8, and carbon signals at δ131.6 and 151.9 were attributed to C-2 and C-3, respectively. Four methyl signals were also observed between δ22.5–17.8. The COSY spectrum showed proton–proton correlations such as H-2 to H-3; H-6 to H-5 and H-7; H-16 to H-15 and H-17; H-11 to H-12; and H-22 to H-23. HMBC spectrum showed pertinent cross-correlation peaks between H-19 and C-1, C-5, C-9, and C-10; H-29 and C-3, C-4, C-5, and C-28; as well as between H-11 and C-8, C-10, C-12, and C-13. The structure of TS1 was determined on the basis of all the above NMR data. The stereochemistry of TS1 was determined with the aid of NOE's correlations as shown in Figure 3B. The coupling constants observed in the ^{1}H NMR spectrum were also very useful. The large coupling constant (J = 12.6 Hz) between H-5 and H-6 clearly showed that both protons were in *trans* position, and the smaller one (J = 3.8 Hz) between H-6 and H-7 was indicative of their *cis* relationship. It is known that in such systems, H-5 is under the plane of the molecule, which automatically means that H-6 is on the upper face of TS1.

TS2 was obtained as white crystals in hexane, mp 212–215°C, $[\alpha]_D^{25}$ + 40.5° (*c* 0.57, $CHCl_3$). The EIMS of TS2 gave a molecular ion peak at *m/z* 506, compatible with the molecular formula $C_{30}H_{34}O_7$. The TS2 IR spectrum showed peaks at 1720 (ester) and 1672 cm^{-1} (enone). The NMR data (Tables 1 and 2) of TS2 were closely related to those of TS1. Additional proton signals were observed in TS2 at δ5.90, 5.67, and 2.00 in ^{1}H NMR spectrum; four additional carbon signals were observed in the ^{13}C NMR spectrum (Table 2) at δ167.1, 137.0, 126.6, and 19.2. HMBC correlation peak observed in TS2 between H-7 and the carbonyl (δ167.1), C-5, C-6, and C-8 indicated that the ester group was linked at C-7. Structure TS2 has thus been assigned on the basis of this spectral data.

Table 1. ^{1}H NMR spectra data for compounds TS1–TS3 ($CDCl_3$, 400 MHz); *J* values in hertz are given in parentheses

H	TS1	TS2	TS3
2	5.93 (d, 9.5)	5.97 (d, 9.5)	5.91 (d, 9.6)
3	7.08 (d, 9.5)	7.09 (d, 9.5)	7.05 (d, 9.6)
5	2.93 (d, 12.6)	2.92 (d, 12.6)	3.35, s
6	4.40 (dd, 12.6, 3.8)	4.47 (dd, 12.6, 4.0)	—
7	3.95 (d, 3.8)	5.51 (d, 4.0)	4.75, s
11	3.81 (dd, 6.4, 1.5)	3.97 (dd, 6.4, 1.4)	3.6 (dd, 5.6, 1.3)
12	1.94, 1.88, m	1.94, 1.88, m	1.95, 1.78, m
15	3.43 (dd, 8.8, 2.9)	3.45 (dd, 8.8, 3.0)	3.30 (dd, 8.8, 2.9)
16	2.20, 1.90, m	2.19, 1.59, m	2.22, 1.88, m
17	2.60 (dd, 11.2, 6.7)	2.54 (dd, 11.3, 6.5)	2.60 (dd, 11.2, 6.7)
18	0.80, s	0.78, s	0.78, s
19	1.41, s	1.44, s	1.41, s
21	7.13, s	7.05, s	7.12, s
22	6.18 (d, 1.6)	6.10, (d, 1.6)	6.15 (d, 1.6)
23	7.36 (d, 1.6)	7.35 (d, 1.6)	7.36 (d, 1.6)
28	3.88, 3.75 (d, 7.3)	3.80, 3.59 (d, 7.3)	4.05, 3.92 (d, 7.2)
29	1.37, s	1.39, s	1.34, s
30	1.10, s	1.30, s	1.18, s
3′	—	2.00, s	—
4′	—	5.90, 5.67 (d, 2)	—

TS3 was obtained as white crystals in hexane, mp 260–262°C, $[\alpha]_D^{25} - 40.5°$ (*c* 0.6, $CHCl_3$). The EIMS for TS3 gave a molecular ion peak at *m/z* 420, compatible with molecular formula $C_{26}H_{28}O_5$. The TS3 IR spectrum showed peaks at 1680 and 1634 cm^{-1}. The NMR data (Tables 1 and 2) of TS3 were again closely related to those of TS1. The hydroxyl group present in the IR spectrum of TS1 was absent in that of TS3, while additional sp^2 carbon atoms appeared in the ^{13}C NMR spectrum of TS3 at δ150.4 and 100.7. This clearly showed that dehydration occurred in TS1 to give TS3. The proposed structure was in agreement with correlations observed in COSY, NOE's, HMQC, and HMBC spectra.

Cell Culture

Fischer rat thyroid (FRT) cell lines stably expressing either CFTR or CFTRΔF508 were a generous gift from M. Welsh (University of Iowa) (28). FRT cells were maintained at 37°C in a humidified, 5% carbon dioxide atmosphere. Growth medium was Coon's modification of Ham's F-12 (Sigma Chemical Co., St. Louis, MO, USA) supplemented with 5% Fetal Bovine Serum (Summit Biotechnology, Ft. Collins, CO, USA) and 100 U/ml of penicillin G sodium, 100 U/ml of streptomycin sulfate, and 0.25 μg/ml of amphotericin B (GibcoBRL, Grand Island, NY, USA).

Electrophysiology

For functional studies, FRT cell lines stably expressing CFTR variants were plated at 2.5×10^5 cells/cm^2 on Millicell-HA cell culture inserts (pore size 0.45 μm, Millipore Co., Bedford, MA, USA) and incubated under the conditions described above. Transepithelial resistance was monitored daily (Millicell Electrical Resistance System, Millipore) and were typically higher than 3000 Ω/cm^2 after 4 days. FRT monolayers were mounted on modified Ussing chambers (Jim's Instruments, Iowa City, IA, USA) and continually gassed with O_2. Temperature was maintained at 37°C. Transepithelial chloride gradient was imposed by bathing the basolateral surface containing (in mM): 135 NaCl, 1.2 $CaCl_2$, 1.2 $MgCl_2$, 2.4 K_2HPO_4, 0.6 KH_2PO_4, 10 HEPES and 10 dextrose, pH 7.4, and the apical surface with a similar solution, except that 135 mM sodium gluconate replaced the 135 mM NaCl, bringing the chloride concentration to 4.8 mM. Under these conditions, the chloride resting potential, according to Nernst equation is 90 mV. The potential difference and the fluid resistance between the potential sensing electrodes were compensated. The transepithelial voltage was

Table 2. ^{13}C NMR spectra data for compounds TS1–TS3 ($CDCl_3$, 100 MHz)

C	TS1	TS2	TS3
1	200.8	200.6	199.5
2	131.6	131.6	132.5
3	151.9	152.0	149.9
4	43.0	43.1	44.2
5	48.8	51.0	54.9
6	73.7	71.5	150.4
7	74.5	75.5	100.7
8	45.5	45.2	41.1
9	65.3	64.9	66.9
10	47.8	47.8	47.5
11	61.0	60.7	59.0
12	35.9	35.7	34.5
13	41.8	41.8	41.5
14	69.9	68.7	72.0
15	55.9	55.6	53.8
16	31.8	31.5	31.2
17	39.7	39.2	40.5
18	21.4	21.5	19.0
19	17.8	17.7	19.2
20	123.9	123.4	123.5
21	139.8	139.7	139.8
22	111.6	111.2	111.3
23	143.1	143.3	143.3
28	80.1	79.9	81.3
29	21.9	22.0	21.6
30	22.5	23.1	24.0
1′	—	167.1	—
2′	—	137.0	—
3′	—	19.2	—
4′	—	126.6	—

clamped to zero (Voltage Clamp Channel Module, model 558C-5, Dept. of Bioengineering, University of Iowa), transepithelial resistance was monitored by recording of current deflections in response to 2-sec pulse of 1–5 mV every 50 sec. The short circuit currents were recorded continuously on a charter recorder (Model SR6335, Western Graphtec, Inc., Irvine, CA, USA). After a stable baseline current was observed (usually within less than 10 min), the channel was activated with cAMP agonists and the current reflecting the flow of Cl^- promoted by its concentration gradient (I_{sc}) was recorded as downward deflection. The I_{sc} was calculated as the difference between the sustained phase of the response and the baseline. Current values were normalized by the area of the insert (0.6 cm^2) and results were expressed in $\mu A/cm^2$.

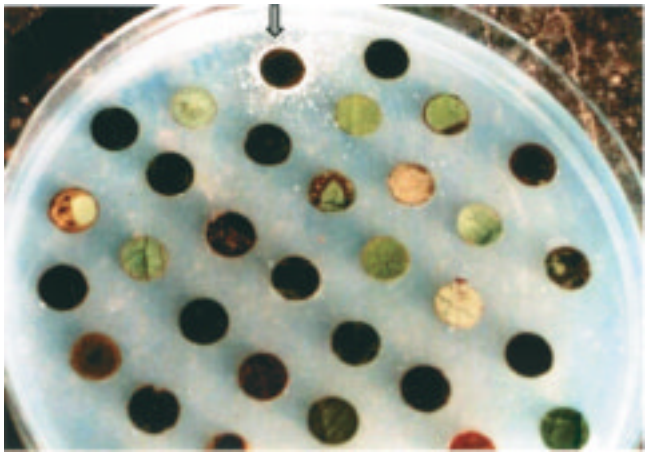

Fig. 2. Yeast two-hybrid assay. Leaf discs were placed on a lawn of YRG2-ΔF spread on Sc –Leu –Trp –His agar media supplemented with 1.5 mM AT. The plate was incubated for 3 days at 30°C. The arrow indicates growth of YRG2-ΔF around the only leaf disc yielding a positive result among the samples tested in this plate (*Trichilia* sp. c.f. *rubescens* Oliv.).

Results

Yeast Two-Hybrid Analysis Shows That CFTR NBD1 Forms Homodimers In Vivo and CF Mutations Affecting CFTR Processing Disrupt This Interaction

Using the yeast two-hybrid system (29), we tested whether CFTR NBD1, in the absence of other CFTR domains, could form homodimers and thereby activate transcription of the HIS3 reporter gene. CFTR NBD1 and the upstream linker region between the first transmembrane domain and NBD1 (aa residues 351–650) were fused in frame with the GAL4 activation domain (AD) and with the GAL4 DNA binding domain (BD), resulting in plasmids pADNBD1 and pBDNBD1, respectively. Cotransformation of the yeast strain YRG-2 with both plasmids (to produce YRG2-WT) conferred a HIS+ phenotype to the yeast, indicating that NBD1 is competent to form homodimers in vivo (Fig. 1). To assess the effect of CF-causing mutations on NBD1 homodimerization, ΔI507, ΔF508, S549R, and G551D were each introduced into NBD1 in both pADNBD1 and pBDNBD1. As shown in Figure 1B, the mutations ΔF508, ΔI507, and S549R, resulted in a HIS- phenotype, indicating defective NBD1 dimerization. The CF-causing mutation G551D, which impairs chloride channel function, but not processing of CFTR, did not result in defective NBD1 dimerization in yeast (Fig. 1).

Use of the Yeast Two-Hybrid System to Screen for Compounds That Restore NBD1ΔF508 Dimerization in Yeast

The results presented suggest that mutations in NBD1 that affect CFTR processing are effectively modeled in yeast. Accordingly, we reasoned that a yeast strain containing derivatives of plasmids pADNBD1 and pBDNBD1 with the ΔF508 mutation

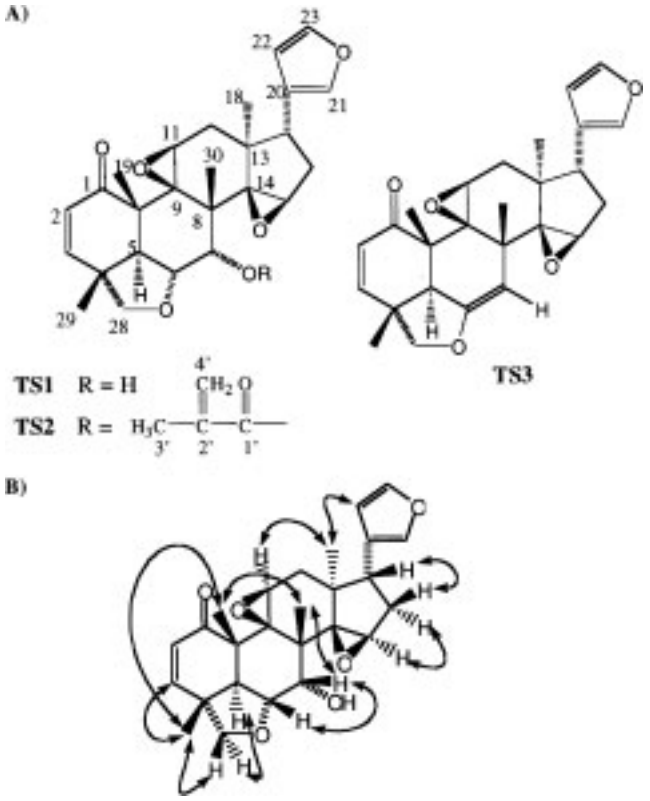

Fig. 3. Purified limonoid compounds from *Trichilia* sp. c.f. *rubescens* Oliv. (A) The structure and stereochemistry of TS1, TS2, and TS3 were determined by analysis of the ^{1}H NMR spectra (Table 1), ^{13}C NMR spectra (Table 2), and IR spectra as described in Materials and Methods. **(B)** NOE's correlation of TS1.

(YRG2-ΔF) would have potential as a drug-screening tool in the identification of new small molecules that restore mutant NBD1 folding and/or dimerization and promote growth of YRG2-ΔF on selective medium. As a source of diverse small molecules for drug screening, we investigated natural product compounds present in plants. Plants are rich in chemical diversity and are an established source of active pharmacologic compounds (30). Direct testing of plant leaf material using the yeast two-hybrid assay allowed large numbers of samples to be screened at a relatively low cost as compared to synthetic chemical libraries. A paper punch was used to sample plant leaves of approximately 600 different species within a segment of tropical rainforest in the Korup National Park of Cameroon. The plant leaf discs were placed in an array on a lawn of YRG2-ΔF yeast in a plate containing selective medium lacking histidine (Fig. 2). Small molecules within the plant discs diffused through the agar into the YRG2-ΔF yeast strain, and compounds with activity to enhance the folding of mutant NBD1, or to enhance mutant NBD1 dimerization, promoted growth of the yeast on selective medium lacking histidine. A plant of the genus *Trichilia* sp. c.f. *rubescens* Oliv. (Meliaceae) was identified as one of eight species testing positive in the bioassay (Fig. 2).

Isolation of Novel Limonoid Compounds That Restore Dimerization to NBD1ΔF508

Leaf material from *Trichilia* sp. c.f. *rubescens* Oliv. was fractionated using the YRG2-ΔF bioassay to direct the purification of the active compound(s). Three structurally related limonoid compounds, designated TS1, TS2, and TS3, were subsequently purified and the structure of each determined by spectroscopic analysis including 2D NMR techniques, as described in Materials and Methods (Tables 1 and 2, Fig. 3). Each purified limonoid compound was tested using the YRG2-ΔF yeast strain (Fig. 4A) and also a control yeast strain in which the NBD1 domain was absent from the GAL4 fusion construct (Fig. 4B). TS3 demonstrated a robust activity in the YRG2-ΔF yeast bioassay; comparatively lower activity was associated with TS2, and no activity was

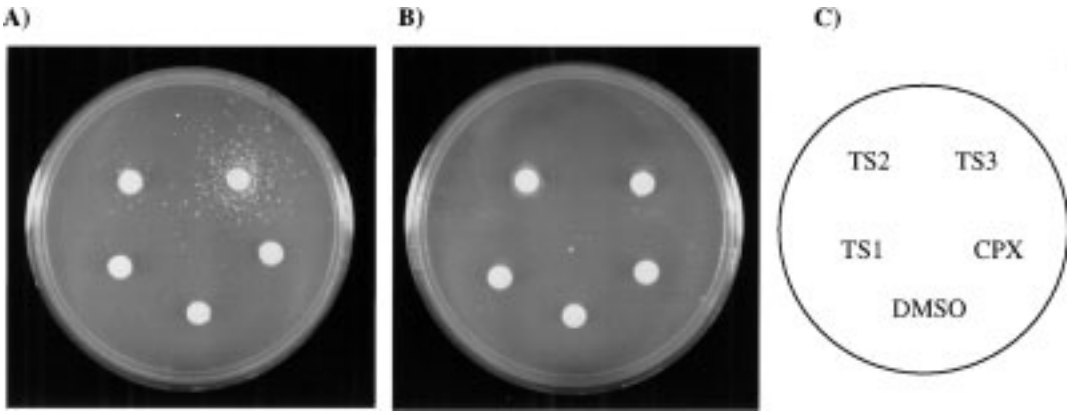

Fig. 4. Activity of the purified compounds TS1, TS2, and TS3 on the yeast two-hybrid assay. 5×10^5 cells of the YRG2-ΔF **(A)** or YRG-2 control strain **(B)** were spread over a selective –His –Leu –Trp plate, supplemented with 5 mM AT. Filter-paper discs containing 5 μl of a 15 mM stock solution of each compound in DMSO was placed on each plate at the position indicated in the diagram **(C)**. Fifteen mM CPX and DMSO were used as controls. Plates were incubated for three days at 30°C.

detected for TS1 (Fig. 4A). CPX (8-cyclopentyl-1, 3-dipropylxanthine), a CFTR activator (31) shown to interact with NBD1 of CFTRΔF508 (32), did not present a detectable activity in the yeast bioassay (Fig. 4A). TS1, TS2, and TS3 did not promote growth of the control yeast strain (Fig. 4B), indicating that the effect of TS2 and TS3 observed for YRG2-ΔF is mediated by the NBDs. TS2 and TS3 also did not affect the growth of YRG2-WT (data not shown), however, wild-type NBD1 dimerizes readily in this strain (resulting in a strong HIS+ phenotype), which may have precluded detection of a growth effect mediated by these compounds. Although the mechanism of action of TS2 and TS3 in correcting the YRG2-ΔF growth defect is unknown, we hypothesized that these compounds could possibly act as chemical chaperones, interacting with and facilitating the folding of NBD1ΔF508 and restoring the NBD1 interaction. The purified limonoids were therefore tested for rescue of the low chloride permeability defect presented by cells expressing CFTRΔF508.

The Limonoid TS3 Is Effective in Increasing the Chloride Permeability of FRT Monolayers Expressing CFTRΔF508

We tested the effect of TS1, TS2, and TS3 in correcting defective cAMP-stimulated chloride permeability in FRT cells stably expressing CFTRΔF508 (FRT-ΔF). Treatment periods longer than 24 hr are usually necessary for assessment of the efficacy of interventions designated to rescue the CFTRΔF508 processing defect. Polarized FRT-ΔF monolayers were incubated for 48 hr in the presence of a range of concentrations of each limonoid compound to assess toxicity. TS2 was the most toxic of the three compounds, leading to decreased transepithelial resistance ($<$170 Ohms/cm^2) of polarized FRT monolayers at concentrations higher than 2 μM. TS1 and TS3 were toxic at concentrations higher than 10 μM. To test the effect of TS1, TS2, and TS3 on the functional activity of CFTRΔF508, monolayers of polarized FRT cells expressing CFTRΔF508 (FRT-ΔF) were incubated in the presence of subtoxic concentrations of each compound for 48 hr and the transepithelial chloride currents were assayed in Ussing chambers, following stimulation with cAMP agonists. In control experiments, FRT-ΔF monolayers were treated with equivalent concentration of DMSO. A low level of cAMP-stimulated chloride current was observed for the FRT-ΔF cell line, approximately 2.5 μA/cm^2 (Fig. 5A). Treatment of FRT-ΔF monolayers with 1–5 μM TS1 or 0.5–2 μM TS2 was without effect on the cAMP-stimulated chloride currents (data not shown). Treatment of FRT-ΔF monolayers for 48 hr with 1 or 5 μM TS3 resulted in 38% and 27% increases, respectively, over DMSO-treated control monolayers (Fig. 5A). Longer incubation of monolayers with 5 μM TS3 for 48–72 hr gave similar results (data not shown). Thus TS3, the limonoid compound that had the greatest potency in correcting the growth defect of the YRG2-ΔF yeast strain, also had a significant effect in increasing the cAMP-stimulated chloride channel current of mammalian cells expressing CFTRΔF508. TS3 had no effect on cAMP-stimulated chloride currents of FRT monolayers not expressing CFTR (Fig. 8).

To establish the duration of the TS3-mediated enhancement of CFTRΔF508 chloride current following removal of the TS3 compound from treated cells ("wash out"), transepithelial currents were measured from TS3-treated monolayers after incubation in compound-free medium for increasing periods of time. As expected, prolonged incubation of TS3-treated monolayers in TS3-free growth medium (24 hr) resulted in a gradual decrease of chloride current, down to control values (Fig. 5A). However, when monolayers were treated with 5 μM TS3 for 48 hr followed by removal of TS3 from the growth medium for only 9 hr, the cAMP-stimulated chloride currents were increased to 1.8-fold relative to control monolayers, a value greater than the 37% increase observed in the absence of the "wash out" (Fig. 5). These results indicate that enhancement of cAMP-stimulated chloride channel conductance by TS3 is further increased by the removal of TS3 prior to measurements of chloride channel conductance.

TS3 Has a Modest Effect in Increasing Chloride Permeability of FRT Monolayers Expressing Wild-Type CFTR

To determine if the effect of TS3 was specific to CFTRΔF508, we incubated FRT monolayers stably expressing wild-type CFTR (FRT-WT) in the presence of 5 μM TS3 for 48 hr and measured the cAMP-activated transepithelial chloride current. TS3 treatment increased the chloride current of monolayers expressing wild-type CFTR (CFTR wt) by 19% over control monolayers (Fig. 6). Incubation of TS3-treated FRT-WT monolayers in TS3-free medium for 9 hr did not result in further increase of the chloride currents (Fig. 6).

Effect of TS3 on CFTR and CFTRΔF508 Chloride Channel Function

Results in Figure 5 indicate that 5 μM TS3 could have a positive effect on CFTRΔF508 processing and an inhibitory effect on chloride channel function. To directly test if TS3 could inhibit CFTR channels, FRT-ΔF and FRT-WT polarized monolayers were incubated for 6 hr in the presence of 5 μM TS3, a period shorter than necessary to detect a possible rescue of the defective processing, but presumably sufficient to allow intracellular accumulation of TS3. The TS3 treatment for 6 hr resulted in a significant inhibition of the CFTRΔF508 chloride currents, to 33% of the control (Fig. 7). The chloride currents of CFTR wt were inhibited to a lesser extent, to 79% of control. TS3 thus partially inhibited both CFTR wt and CFTRΔF508 function when present

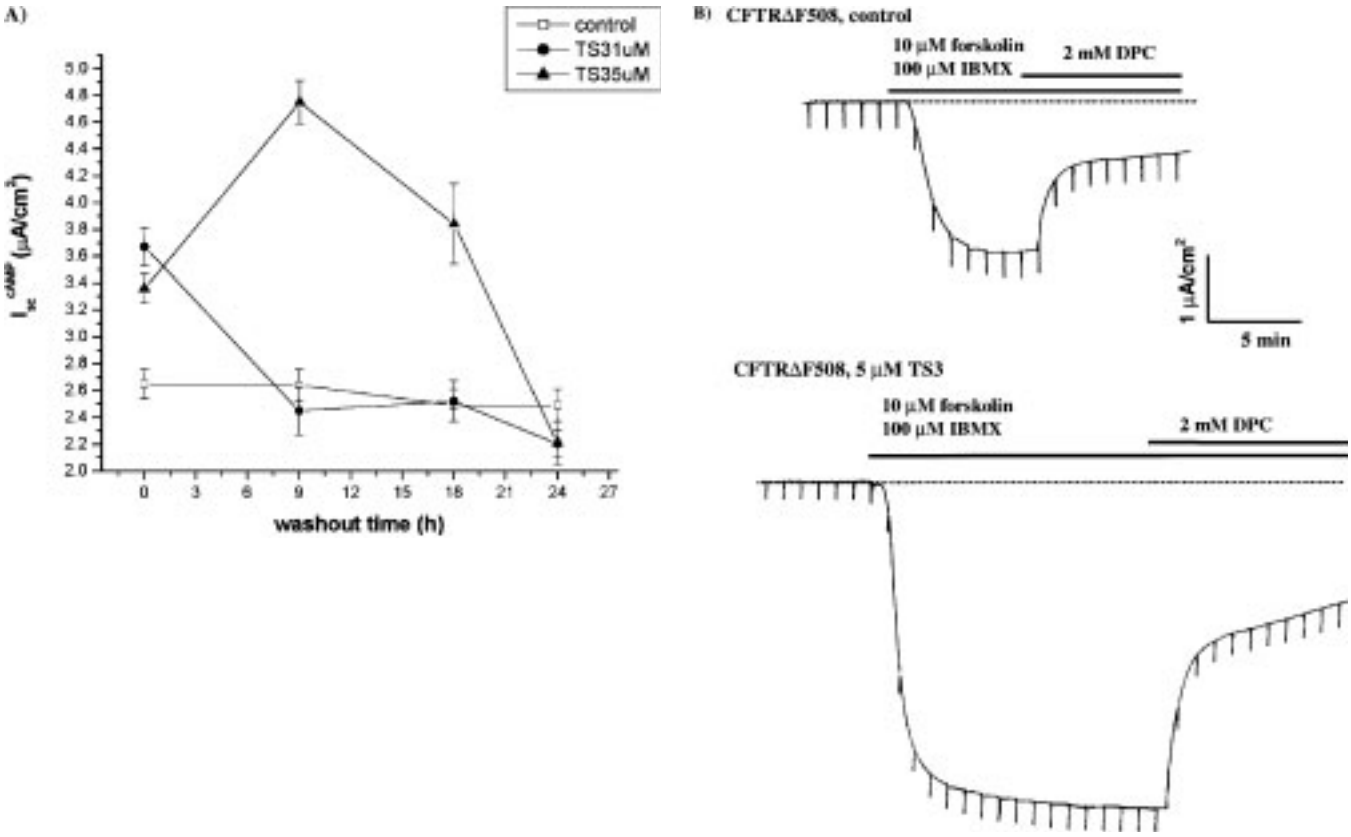

Fig. 5. Effect of TS3 on CFTRΔF508 mediated cAMP-activated chloride current. (A) Polarized monolayers of FRT cells expressing CFTRΔF508 were incubated for 48 hr with TS3 (1 or 5 μM, as indicated) or the equivalent amount of DMSO. The monolayers were subsequently incubated in TS3-free growth medium for the time (hr) indicated, mounted in Ussing chambers, and transepithelial chloride currents were measured after activation with 10 μM forskolin and 100 μM IBMX. Results represent the mean ±SEM for the number of experiments (n) indicated. Five μM TS3 treatment resulted in a significant difference from the respective control ($p < 0.01$, two-tailed t-test) for wash out time points 0 hr ($n = 4$), 9 hr ($n = 15$), and 18 hr ($n = 3$). One μM TS3 treatment resulted in a significant difference from the respective control ($p < 0.01$, two-tailed t-test) for wash out time point 0 hr ($n = 4$). For all other time points $n = 4$ (or greater). **(B)** Representative tracing for control and 5 μM TS3-treated cells after 9 hr of incubation in TS3-free growth medium. The bars indicate the presence of cAMP agonists (10 μM forskolin and 100 μM IBMX) and CFTR inhibitor (2 mM DPC). The dashed line represents the baseline current, before activation with cAMP agonists.

for a short incubation period that would preclude a possible positive effect on processing.

Addition of 5–15 μM TS3 directly to FRT-ΔF monolayers mounted in Ussing chambers, either before or after stimulation with cAMP agonists, did not increase CFTRΔF508 chloride current (data not shown), nor did a short incubation of FRT-ΔF monolayers with TS3 for only 6 hr (Fig. 7). These results, taken together with the results shown in Figure 5, suggest that the effect of TS3 to increase chloride conductance of cells expressing CFTRΔF508 is not immediate as observed with CFTR channel activators such as CPX and genistein (32–34), and is more likely to result in a time-dependent effect on CFTR processing rather than function. However, we were unable to detect in a Western blot an increase in the amount of the fully glycosylated form of CFTRΔF508 in response to incubation of the cells with TS3 (data not shown), indicating that enhancement of processing by TS3 is small.

TS3 Treatment Combined With Genistein Activation Effectively Rescues the Chloride Impermeability of FRT-ΔF

Genistein is an activator of CFTR that has been shown to increase the open time probability P_o of the CFTRΔF508 channel (13,18,35). The presence of 50 μM of genistein during chloride channel activation significantly enhances chloride currents of DMSO- and TS3-treated FRT-ΔF monolayers by 100% and 51%, respectively (Fig. 8). A 3-fold increase in chloride channel conductance in FRT-ΔF cells is obtained when 50 μM of genistein is used to activate TS3-treated monolayers (Fig. 8). The effects of TS3 and genistein are thus additive, suggesting that enhanced restoration of CFTRΔF508 functional activity can be attained with the use of small molecules having complementary effects in restoring CFTRΔF508 processing and function. Furthermore, the magnitude of the CFTRΔF508 chloride current increase resulting from 5 μM TS3 treatment was similar to the effect of activation with 50 μM genistein alone (Fig. 8).

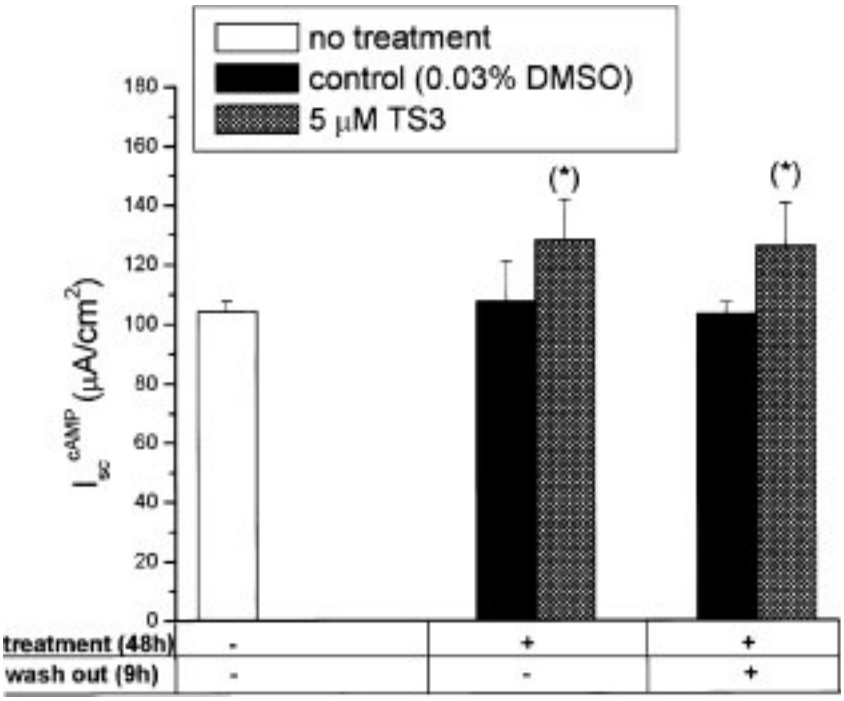

Fig. 6. Effect of TS3 on wildtype CFTR mediated cAMP activated chloride current. Polarized monolayers of FRT cells expressing CFTR wt (FRT-WT) were incubated for 48 hours with 5 μM TS3 or the equivalent amount of DMSO (control). In some experiments, the monolayers were subsequently incubated for 9 hours in TS3-free growth medium. Monolayers were mounted in Ussing chambers and transepithelial chloride currents were measured after activation with 10 μM forskolin and 100 μM IBMX. Results represent the mean ±SEM of n = 6 experiments. The asterisk indicates that the TS3 treatment resulted in a significant difference from the respective control ($p < 0.05$, two-tailed *t*-test).

Discussion

The molecular basis for the effect of the ΔF508 mutation on CFTR processing is unknown, although it is generally accepted that the mutation causes misfolding of the CFTRΔF508 polypeptide within the ER (36), resulting in retention and degradation by the ER-associated quality control mechanism (37) and substantially reduced levels of CFTRΔF508 at the plasma membrane. CFTRΔF508 that is correctly located at the plasma membrane has decreased stability in relation to CFTR wt (38–40); however, the mutant protein still retains at least one-third of the chloride channel activity of wild-type CFTR (14).

Using the yeast two-hybrid system, we have determined that CFTR NBD1 forms dimers in vivo in yeast and that ΔF508 impairs the ability of NBD1 to

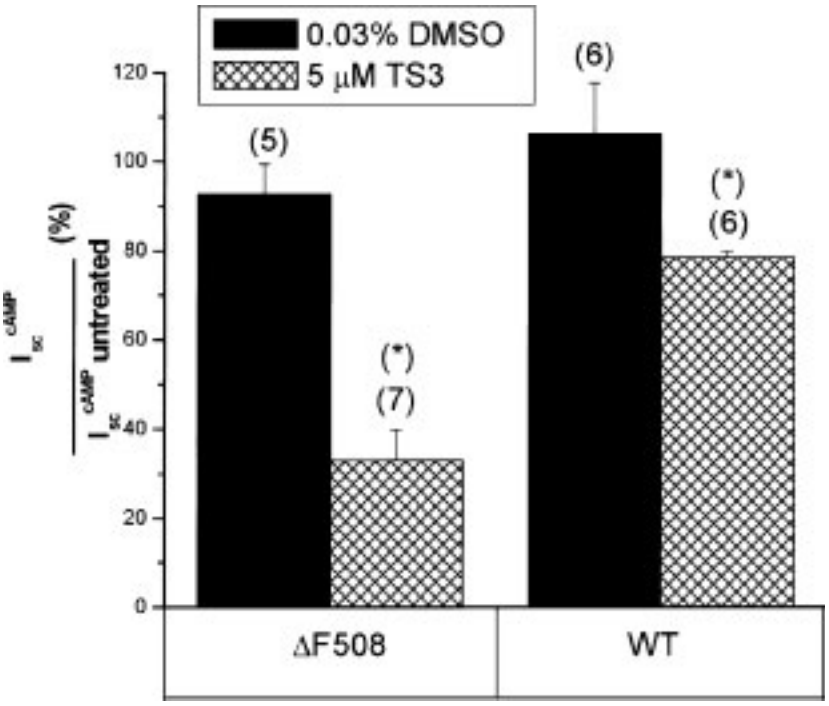

Fig. 7. Effect of short-term TS3 treatment of cells on cAMP activated chloride channel function of CFTRΔF508 or wildtype CFTR. Polarized monolayers of FRT-ΔF cells expressing CFTRΔF508 (ΔF508) or FRT-WT cells expressing CFTR wt (WT) were incubated for 6 hours with 5 μM TS3 or the equivalent amount of DMSO (0.03%). Monolayers were mounted in Ussing chambers and transepithelial chloride currents were measured after activation with 10 μM forskolin and 100 μM IBMX. The maximal cAMP-stimulated chloride conductance observed for untreated FRT-WT monolayers was 85 μA/cm^2. Results are expressed as percentage of currents for untreated monolayers and represent the mean ±SEM for the indicated number of experiments (*n*). The asterisk indicates that the TS3 treatment resulted in a significant difference from the respective control ($p < 0.05$, two-tailed *t*-test).

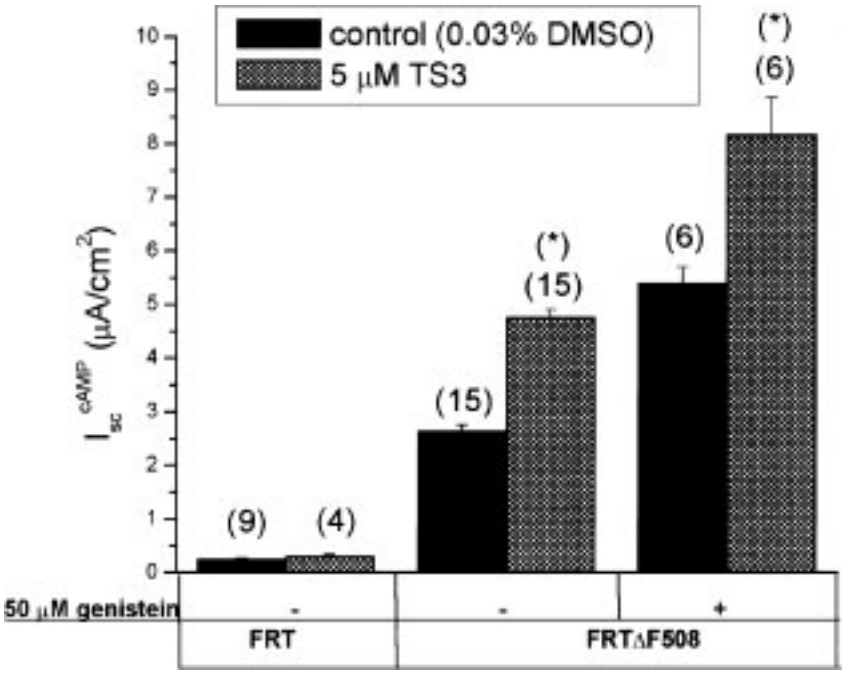

Fig. 8. The combined effect of TS3 and genistein to increase CFTRΔF508 cAMP-activated chloride current. Polarized monolayers of FRT cells (FRT) or FRT-ΔF cells expressing CFTRΔF508 (FRT-ΔF508) were incubated for 48 hours with 5 μM TS3 or the equivalent amount of DMSO and subsequently incubated for 9 hours in TS3-free growth medium. Monolayers were mounted in Ussing chambers and transepithelial chloride currents were measured after activation with 10 μM forskolin and 100 μM IBMX or with 50 μM genistein followed by 10 μM forskolin and 100 μM IBMX, as indicated. Results represent the mean ±SEM for the indicated number of experiments (n). The asterisks indicate that TS3 treatment resulted in a significant increase in chloride current ($p < 0.01$, two-tailed t-test).

form dimers. Because dimerization of NBDs has been demonstrated for several other ABC transporters (22,25,26,41–43), the dimerization of NBD1 that we observe in yeast may represent a bona fide interaction between NBD1 domains of CFTR molecules that occurs in vivo in mammalian cells during the normal processing of CFTR. The quaternary structure of CFTR is currently a subject of debate, although previous experiments have suggested that CFTR is a monomer (44). Recently, however, it has been shown that CFTR has the appearance of dimers at the plasma membrane (45) and in reconstituted liposomes (46). Dimerization has also been shown to regulate CFTR functional activity (47). The dimeric form may thus be transient and represent only a fraction of the CFTR within the cell.

Our results indicate that CFTR processing is associated with folding of wild-type NBD1 into a structure that is competent to form homodimers. CF mutations affecting CFTR processing (ΔF508, ΔI507, and S549R) resulted in defective CFTR NBD1 dimer formation in yeast. In contrast, the G551D mutation, which does not impair CFTR processing, had no effect on NBD1 association. The correlation between mutations causing defective processing of CFTR and defective dimerization of NBD1 in yeast further suggests that dimerization of CFTR, mediated in part by NBD1, could be associated with CFTR processing. Alternatively, it is possible that NBD1 dimer formation is a property of NBD1 that has folded into a native state, thereby becoming competent to self-associate. Interestingly, dimerization of the NBD domains of peroxisomal ABC "half-transporters" have also been shown in the yeast two-hybrid system, and dimerization was disrupted by two mutations associated with X-linked adrenoleukodystrophy (43). Homodimerization of NBD1 in yeast could be a consequence of the absence of NBD2 because allosteric interaction between NBD1 and NBD2 has been observed (48). However, interaction between NBD1 and NBD2 using the yeast two-hybrid system has not been observed (49).

Although the biological significance of CFTR NBD1 dimerization in vivo is unknown, the yeast two-hybrid assay provides a means to assay a growth-defective phenotype for a CF-causing mutation in yeast, and to detect the activity of bioactive small molecules that reverse the growth defect. We have used this assay to screen a biodiverse collection of tropical plants. Bioassay-directed fractionation from *Trichilia* sp. c.f. *rubescens* Oliv. yielded a pure limonoid compound TS3 with activity to correct the growth defect of YRG2-ΔF. Limonoids are a group of highly oxidized terpenoids present in several species of the genus *Trichilia* (50–57). Several biological activities have been shown for limonoid compounds: insect antifeedant (58–60), inhibition of cell adhesion (61), toxicity to DNA repair deficient yeast (62), and antimicrobial activity (63). Possibly other limonoids from related *Trichilia* species or derivatives of TS3 have activity to correct the ΔF508 defect. Because TS3 demonstrated activity to correct both the ΔF508 growth defect in yeast and also the chloride permeability defect in FRT-ΔF cells, the results strongly suggest that the effect of the ΔF508 mutation on NBD1 is effectively modeled in yeast, and that activity of compounds to correct the molecular defect may be assayed using the yeast two-hybrid system.

Enhancement of CFTRΔF508 chloride current by TS3 treatment was increased when the cells were incubated in TS3-free medium prior to measurement of chloride conductance. These results lead us to hypothesize that increased chloride conductance resulting from a putative positive effect of TS3 to increase CFTRΔF508 levels at the plasma membrane may be countered by an inhibitory effect of TS3 on CFTRΔF508 function. In support of this notion, an inhibitory effect of TS3 was also noted when FRT-ΔF monolayers were incubated with 5 μM TS3 for 6 hr. We did not observe enhancement of CFTRΔF508 chloride current in CFTR cells expressing CFTRΔF508 when cells were incubated with limonoid compounds TS1 or TS2. As shown in Figure 3A, these compounds differ from TS3 only with respect to the functional group associated with C7 position, which is hydrogen in TS3. This suggests that the activity of TS3 to correct the NBD1 dimerization defect in yeast and also the activity to enhance chloride conductance from cells expressing CFTRΔF508 depends at least in part on the structural determinants presented at C7.

TS3-mediated increase in FRT-ΔF chloride currents required that monolayers were incubated for at least 48 hr with TS3, consistent with the time required to detect the functional activity associated with an increase in processed CFTRΔF508. In contrast, short incubations of FRT-ΔF cells with TS3 for periods of 6 hr or less did not result in a TS3-mediated increase in FRT-ΔF chloride current. The TS3 compound therefore does not appear to activate CFTRΔF508 in the same manner as genistein or CPX, which induce a rapid increase in the functional activity of CFTRΔF508 already localized at the plasma membrane. Instead, TS3 most likely promotes an increase of CFTRΔF508 channels at the plasma membrane, detectable as an increase in cAMP-stimulated chloride currents, which could result from improved processing at the ER or increased stability of the small fraction of the mutant protein present at the plasma membrane. A TS3-mediated increase in the amount of processed CFTRΔF508 at the plasma membrane was not detected by Western blot analysis, suggesting that the effect of TS3 to correct processing is small. However, in analogous studies involving treatment of MDCK cells expressing CFTRΔF508 with the anticancer drug doxorubicin, it was similarly observed that a drug-mediated increase in cAMP-stimulated chloride channel activity (64) corresponded to only a small improvement of CFTRΔF508 processing, which was not readily detectable by Western blot analysis.

It has been estimated that 10% of wild-type CFTR activity can rescue the electrolyte defect in a CF tissue (65), representing roughly a 10-fold increase in CFTRΔF508-mediated chloride permeability. TS3 did not mediate this level of rescue of CFTRΔF508; however, a 3-fold increase in the cAMP-stimulated chloride current in FRT cells expressing CFTRΔF508 was attained by treatment with both genistein and TS3. An effective strategy to increase CFTRΔF508 chloride conductance may thus involve a combination of small molecules that are active in rescuing CFTRΔF508 processing and functional defects. TS3 represents a novel class of compounds that can interact with NBD1 ΔF508 in vivo and promote an increase in cAMP-stimulated chloride permeability of cells expressing CFTRΔ508. The yeast two-hybrid assay described here provides a means to identify additional new small molecules that target NBD1 and have activity to increase the chloride permeability of cells expressing CFTRΔF508.

Acknowledgments

We are grateful to the members of the African International Cooperative in Biodiversity Group (ICBG) and the Smithsonian Institute for Tropical Research, especially Liz Losos, Duncan Thomas, Sainge Moses, Mambo Peter, Rodney Stubina, and David Kenfack, for their invaluable help during plant collection and identification. This study was supported by the ICBG "Drug Development and Conservation in West and Central Africa" Grant No TW01023-01-AP2 from the Fogarty Center, NIH, and Grant No CAM:02 from the International Science Program (ISP), Uppsala University, Sweden.

References

1. Riordan JR, Rommens JM, Kerem B, et al. (1989) Identification of the cystic fibrosis gene: cloning and characterization of complementary DNA [published erratum appears in *Science* (1989) **245**:1437]. *Science* **245**: 1066–1073.
2. Rommens JM, Iannuzzi MC, Kerem B, et al. (1989) Identification of the cystic fibrosis gene: chromosome walking and jumping. *Science* **245**: 1059–1065.
3. Welsh MJ, Smith AE. (1993) Molecular mechanisms of CFTR chloride channel dysfunction in cystic fibrosis. *Cell* **73**:1251–1254.
4. Sheppard DN, Welsh MJ. (1999) Structure and function of the CFTR chloride channel. *Physiol. Rev.* **79(suppl 1)**: S23–S45.
5. Holland IB, Blight MA. (1999) ABC-ATPases, adaptable energy generators fuelling transmembrane movement of a variety of molecules in organisms from bacteria to humans. *J. Mol. Biol.* **293**: 381–399.
6. Higgins CF. (1992) ABC transporters: From microorganisms to man. *Annu. Rev. Cell Biol.* **8**: 67–113.
7. Jensen TJ, Loo MA, Pind S, Williams DB, Goldberg AL, Riordan JR. (1995) Multiple proteolytic systems, including the proteasome, contribute to CFTR processing. *Cell* **83**: 129–135.
8. Lukacs GL, Mohamed A, Kartner N, Chang XB, Riordan JR, Grinstein S. (1994) Conformational maturation of CFTR but not its mutant counterpart (delta F508) occurs in the endoplasmic reticulum and requires ATP. *Embo. J.* **13**: 6076–6086.
9. Meacham GC, Patterson C, Zhang W, Younger JM, Cyr DM. (2001) The Hsc70 co-chaperone CHIP targets immature CFTR for proteasomal degradation. *Nat. Cell Biol.* **3**: 100–105.
10. Pind S, Riordan JR, Williams DB. (1994) Participation of the endoplasmic reticulum chaperone calnexin (p88, IP90) in the biogenesis of the cystic fibrosis transmembrane conductance regulator. *J. Biol. Chem.* **269**: 12784–12788.
11. Ward CL, Omura S, Kopito RR. (1995) Degradation of CFTR by the ubiquitin-proteasome pathway. *Cell* **83**: 121–127.
12. Haws CM, Nepomuceno IB, Krouse ME, Wakelee H, Law T, Xia Y, Nguyen Y, Wine JJ. (1996) Delta F508-CFTR channels:

kinetics, activation by forskolin, and potentiation by xanthines. *Am. J. Physiol.* **270:** C1544–C1555.
13. Hwang TC, Wang F, Yang IC, Reenstra WW. (1997) Genistein potentiates wild-type and delta F508-CFTR channel activity. *Am. J. Physiol.* **273:** C988–C998.
14. Dalemans W, Barbry P, Champigny G, et al. (1991) Altered chloride ion channel kinetics associated with the delta F508 cystic fibrosis mutation [see comments]. *Nature* **354:** 526–528.
15. Sato S, Ward CL, Krouse ME, Wine JJ, Kopito RR. (1996) Glycerol reverses the misfolding phenotype of the most common cystic fibrosis mutation. *J. Biol. Chem.* **271:** 635–638.
16. Brown CR, Hong-Brown LQ, Biwersi J, Verkman AS, Welch WJ. (1996) Chemical chaperones correct the mutant phenotype of the delta F508 cystic fibrosis transmembrane conductance regulator protein. *Cell Stress Chaperones* **1:** 117–125.
17. Denning GM, Anderson MP, Amara JF, Marshall J, Smith AE, Welsh MJ. (1992) Processing of mutant cystic fibrosis transmembrane conductance regulator is temperature-sensitive [see comments]. *Nature* **358:** 761–764.
18. Hwang TC, Sheppard DN. (1999) Molecular pharmacology of the CFTR Cl- channel. *Trends Pharmacol. Sci.* **20:** 448–453.
19. Schultz BD, Singh AK, Devor DC, Bridges RJ. (1999) Pharmacology of CFTR chloride channel activity. *Physiol. Rev.* **79(suppl 1):** S109–S144.
20. Cheng SH, Gregory RJ, Marshall J, Paul S, Souza DW, White GA, O'Riordan CR, Smith AE. (1990) Defective intracellular transport and processing of CFTR is the molecular basis of most cystic fibrosis. *Cell* **63:** 827–834.
21. Thomas PJ, Pedersen PL. (1993) Effects of the delta F508 mutation on the structure, function, and folding of the first nucleotide-binding domain of CFTR. *J. Bioenerg. Biomembr.* **25:** 11–19.
22. Kennedy KA, Traxler B. (1999) MalK forms a dimer independent of its assembly into the MalFGK2 ATP-binding cassette transporter of Escherichia coli. *J. Biol. Chem.* **274:** 6259–6264.
23. Nikaido K, Liu PQ, Ames GF. (1997) Purification and characterization of HisP, the ATP-binding subunit of a traffic ATPase (ABC transporter), the histidine permease of *Salmonella typhimurium*. Solubility, dimerization, and ATPase activity. *J. Biol. Chem.* **272:** 27745–27752.
24. Liu P-Q, Ames GF-L. (1998) In vitro disassembly and reassembly of an ABC transporter, the histidine permease. *Proc. Natl. Acad. Sci. U.S.A.* **95:** 3495–3500.
25. Hung LW, Wang IX, Nikaido K, Liu PQ, Ames GF, Kim SH. (1998) Crystal structure of the ATP-binding subunit of an ABC transporter [see comments]. *Nature* **396:** 703–707.
26. Lapinski PE, Miller GG, Tampe R, Raghavan M. (2000) Pairing of the nucleotide binding domains of the transporter associated with antigen processing. *J. Biol. Chem.* **275:** 6831–6840.
27. Jolad SD, Hoffmann JJ, Schram KH, Cole JR, Tempesta MS. (1981) Constituents of *Trichilia hispida* (Meliaceae). 3. Structures of the cytotoxic limonoids: Hispidins A, B, C. *J. Org. Chem.* **46:** 641–644.
28. Sheppard DN, Carson MR, Ostedgaard LS, Denning GM, Welsh MJ. (1994) Expression of cystic fibrosis transmembrane conductance regulator in a model epithelium. *Am. J. Physiol.* **266:** L405–L413.
29. Fields S, Song O. (1989) A novel genetic system to detect protein-protein interactions. *Nature* **340:** 245–246.
30. Simmonds MSJ, Grayer R. (1999) Drug discovery and development. In Walton NJ, Brown DE, eds. *Chemicals from Plants: Perspectives on Plant Secondary Products*. River Edge, NJ: Imperial College Press; 215–249.
31. Eidelman O, Guay-Broder C, van Galen PJ, et al. (1992) A1 adenosine-receptor antagonists activate chloride efflux from cystic fibrosis cells. *Proc. Natl. Acad. Sci. U.S.A.* **89:** 5562–5566.
32. Cohen BE, Lee G, Jacobson KA, et al. (1997) 8-Cyclopentyl-1,3-dipropylxanthine and other xanthines differentially bind to the wild-type and delta F508 first nucleotide binding fold (NBF-1) domains of the cystic fibrosis transmembrane conductance regulator. *Biochemistry* **36:** 6455–6461.
33. He Z, Raman S, Guo Y, Reenstra WW. (1998) Cystic fibrosis transmembrane conductance regulator activation by cAMP-independent mechanisms. *Am. J. Physiol.* **275:** C958–C966.
34. Al-Nakkash L, Hwang TC. (1999) Activation of wild-type and deltaF508-CFTR by phosphodiesterase inhibitors through cAMP-dependent and -independent mechanisms. *Pflugers Arch.* **437:** 553–561.
35. Wang F, Zeltwanger S, Hu S, Hwang TC. (2000) Deletion of phenylalanine 508 causes attenuated phosphorylation-dependent activation of CFTR chloride channels. *J. Physiol. (Lond)* **524:** 637–648.
36. Zhang F, Kartner N, Lukacs GL. (1998) Limited proteolysis as a probe for arrested conformational maturation of delta F508 CFTR [see comments]. *Nat. Struct. Biol.* **5:** 180–183.
37. Kopito RR. (1999) Biosynthesis and degradation of CFTR. *Physiol. Rev.* **79(suppl 1):** S167–S173.
38. Lukacs GL, Chang XB, Bear C, et al. (1993) The delta F508 mutation decreases the stability of cystic fibrosis transmembrane conductance regulator in the plasma membrane. Determination of functional half-lives on transfected cells. *J. Biol. Chem.* **268:** 21592–21598.
39. Heda GD, Tanwani M, Marino CR. (2001) The Delta F508 mutation shortens the biochemical half-life of plasma membrane CFTR in polarized epithelial cells. *Am. J. Physiol. Cell. Physiol.* **280:** C166–C174.
40. Sharma M, Benharouga M, Hu W, Lukacs GL. (2001) Conformational and temperature-sensitive stability defects of the delta F508 cystic fibrosis transmembrane conductance regulator in post-endoplasmic reticulum compartments. *J. Biol. Chem.* **276:** 8942–8950.
41. Yaan Y, Blecker S, Martsinkevieh O, Miften L, Thomas P, Hant J. (2001) The crystal structure of the MJO796 ATP-binding cassette. Implications for the structural consequences of ATP hydrolysis in the active site of an ABC transporter. *J. Biol. Chem.* **276:** 32313–21.
42. Hopfner KP, Karcher A, Shin DS, et al. (2000) Structural biology of Rad50 ATPase: ATP-driven conformational control in DNA double-strand break repair and the ABC-ATPase superfamily. *Cell* **101:** 789–800.
43. Liu LX, Janvier K, Berteaux-Lecellier V, Cartier N, Benarous R, Aubourg P. (1999) Homo- and heterodimerization of peroxisomal ATP-binding cassette half-transporters. *J. Biol. Chem.* **274:** 32738–32743.
44. Marshall J, Fang S, Ostedgaard LS, et al. (1994) Stoichiometry of recombinant cystic fibrosis transmembrane conductance regulator in epithelial cells and its functional reconstitution into cells in vitro. *J. Biol. Chem.* **269:** 2987–2995.
45. Eskandari S, Wright EM, Kreman M, Starace DM, Zampighi GA. (1998) Structural analysis of cloned plasma membrane proteins by freeze-fracture electron microscopy. *Proc. Natl. Acad. Sci. U.S.A.* **95:** 11235–11240.
46. Ramjeesingh M, Li C, Kogan I, Wang Y, Huan LJ, Bear CE. (2001) A monomer is the minimum functional unit required for channel and ATPase activity of the cystic fibrosis transmembrane conductance regulator. *Biochemistry* **40:** 10700–10706.
47. Wang S, Yue H, Derin RB, Guggino WB, Li M. (2000) Accessory protein facilitated CFTR-CFTR interaction, a molecular mechanism to potentiate the chloride channel activity. *Cell* **103:** 169–179.
48. Ramjeesingh M, Li C, Garami E, et al. (1999) Walker mutations reveal loose relationship between catalytic and channel-gating activities of purified CFTR (cystic fibrosis transmembrane conductance regulator). *Biochemistry* **38:** 1463–1468.
49. Taylor JC, Horvath AR, Higgins CF, Begley GS. (2001) The multidrug resistance p-glycoprotein. Oligomeric state and intramolecular interactions. *J. Biol. Chem.* **276:** 36075–36078.
50. Cortez DA, Fernandes JB, Vieira PC, da Silva MF, Ferreira AG. (2000) A limonoid from *Trichilia estipulata*. *Phytochemistry* **55:** 711–713.
51. Connolly JD, Labbe C, Rycroft DS, Okorie DA, Taylor DAH. (1979) Tetranortriterpenoids and related compounds. Part 23.

Complex tetranortriterpenoids from *Trichilia prieuriana* and *Guarea thompsonii* (Meliaceae), and the hydrolysis products of drageanin, prieurianin, and related compounds. *J. Chem. Res. Synop.* **1979:** 256–257.
52. Arenas C, Rodriguez-Hahn L. (1990) Limonoids from *Trichilia havanensis*. *Phytochemistry* **29:** 2953–2956.
53. Garcez FR, Garcez WS, Tsutsumi MT, Roque NF. (1997) Limonoids from *Trichilia elegans* ssp. *Phytochemistry* **45:** 141–148.
54. Inada A, Konishi M, Murata H, Nakanishi T. (1994) Structures of a new limonoid and a new triterpenoid derivative from pericarps of *Trichilia connaroides. J. Nat. Prod.* **57:** 1446–1449.
55. Olugbade TA, Adesanya SA. (2000) Prieurianoside, a protolimonoid glucoside from the leaves of *Trichilia prieuriana. Phytochemistry* **54:** 867–870.
56. Rodriguez-Hahn L, Cardenas J, Arenas C. (1996) Trichavesin, a prieurianin derivative from *Trichilia havanensis. Phytochemistry* **43:** 457–459.
57. Taylor DAH. (1982) A new structural proposal for the tetranortriterpenoid dregeanin. *J. Chem. Res. Synop.* **1982:** 55.
58. Nakanishi K. (1982) Recent studies on bioactive compounds from plants. *J. Nat. Prod.* **45:** 15–26.
59. Nakatani M, Okamoto M, Iwashita T, Miuzukawa K, Naoki H, Hase T. (1984) Isolation and structures of three secolimonoids, insect antifeedants from *Trichilia roka* (Meliaceae). *Heterocycles* **22:** 2335–2340.
60. Nakatani M, Iwashita T, Naoki H, Hase T. (1985) Structure of a limonoid antifeedant from *Trichilia roka. Phytochemistry* **24:** 195–196.
61. Musza LL, Killar LM, Speight S, et al. (1994) Potent new cell adhesion inhibitory compounds from the root of *Trichilia rubra. Tetrahedron* **50:** 11369–11378.
62. Gunatilaka AA, Bolzani V, Dagne E, et al. (1998) Limonoids showing selective toxicity to DNA repair-deficient yeast and other constituents of *Trichilia emetica. J. Nat. Prod.* **61:** 179–184.
63. Aladesanmi AJ, Odediran SA. (2000) Antimicrobial activity of *Trichilia heudelotti* leaves. *Fitoterapia* **71:** 179–182.
64. Maitra R, Shaw CM, Stanton BA, Hamilton JW. (2001) Increased functional cell surface expression of CFTR and DeltaF508-CFTR by the anthracycline doxorubicin. *Am. J. Physiol. Cell Physiol.* **280:** C1031–C1037.
65. Johnson LG, Olsen JC, Sarkadi B, Moore KL, Swanstrom R, Boucher RC. (1992) Efficiency of gene transfer for restoration of normal airway epithelial function in cystic fibrosis. *Nat. Genet.* **2:** 21–25.

Trypanocidal Diarylheptanoids from *Aframomum letestuianum*

Pierre Kamnaing,[†] Apollinaire Tsopmo,[‡] Eric A. Tanifum,[†] Marguerite H. K. Tchuendem,[†] Pierre Tane,[†] Johnson F. Ayafor,[†,||] Olov Sterner,*[,‡] Donna Rattendi,[§] Maurice M. Iwu,[⊥] Brian Schuster,[⊥] and Cyrus Bacchi*[,§]

Department of Chemistry, University of Dschang, Box 67, Dschang, Cameroon, Department of Organic and Bioorganic Chemistry, Lund University, P.O. Box 124, SE 221 00 Lund, Sweden, Division of Experimental Therapeutics, Walter Reed Army Institute of Research, Washington, D.C. 20307-5100, and Haskins Laboratories and Department of Biology, Pace University, New York, New York 10038-1502

Received August 23, 2002

Three new diarylheptanoids, (4*Z*,6*E*)-5-hydroxy-1-(4-hydroxy-3-methoxyphenyl)-7-(4-hydroxyphenyl)hepta-4,6-dien-3-one, letestuianin A (**1**), (4*Z*,6*E*)-5-hydroxy-1,7-bis(4-hydroxy-3-methoxyphenyl)hepta-4,6-dien-3-one, letestuianin B (**2**), and 1,7-bis(4-hydroxyphenyl)heptan-3,5-dione, letestuianin C (**3**), as well as the known (4*Z*,6*E*)-5-hydroxy-1,7-bis(4-hydroxyphenyl)hepta-4,6-dien-3-one (**5**) were isolated from *Aframomum letestuianum*. The known flavonoids 3-acetoxy-5,7,4′-trihydroxyflavanone, 3-acetoxy-7-methoxy-5,4′-dihydroxyflavanone, 7-methoxy-3,5,4′-trihydroxyflavone, and 3,3′,4′,5,7-pentahydroxyflavan were also obtained from this plant. Their structures were determined using a combination of 1D and 2D NMR techniques. The four diarylheptanoids were tested for growth inhibitory activity in vitro versus bloodstream forms of African trypanosomes. IC_{50} values in the range of 1−3 μg/mL were found for compounds **3** and **5**.

The genus *Aframomum* K. Schum belongs to the economically and medicinally important family Zingiberaceae. It is represented in Cameroon by over 20 species of rhizomatous herbs.[1] All of them are widely used locally in ethnodietary and in folk medicinal preparations as well as for cultural and spiritual purposes.[2] In our previous research on this genus, we reported the isolation and characterization of several flavonoids and labdane diterpenes.[3−5] In continuation of our work on this genus and as part of our efforts to discover new antiparasitic drug leads from Cameroonian medicinal plants[6] we have investigated the seeds of *Aframomum letestuianum* and herein report the isolation of four diarylheptanoids. Three are new compounds to which we have given the trivial names letestuianin A (**1**), letestuianin B (**2**), and letestuianin C (**3**). The fourth is the previously reported (4*Z*,6*E*)-5-hydroxy-1,7-bis(4-hydroxyphenyl)hepta-4,6-dien-3-one (**5**).[7] In addition, the known flavonoids 3-acetoxy-5,7,4′-trihydroxyflavanone,[4] 3-acetoxy-7-methoxy-5,4′-dihydroxyflavanone,[4] 7-methoxy-3,5,4′-trihydroxyflavone,[5] and 3,3′,4′,5,7-pentahydroxyflavan[8] were isolated in large quantitities. The trypanocidal activity of the diarylheptanoids is presented.

Results and Discussion

A sample of the air-dried powdered seeds of *A. lestestuianum* was extracted with MeOH−CH_2Cl_2 and subjected to sequential extraction with hexane and CH_2Cl_2. Bioassay-guided fractionation and purification of the CH_2Cl_2-soluble fractions led to the isolation of four diarylheptanoids and four flavonoids. The structures of the compounds were elucidated by spectroscopic techniques, and comparison with literature data revealed that three of the isolated diarylheptanoids are new compounds.

Compound **1** was obtained as a yellowish oil. The EIMS spectrum showed a molecular ion peak at *m*/*z* 340 with 100% intensity, compatible with the molecular formula $C_{20}H_{20}O_5$. The IR spectrum showed important absorption bands at ν_{max} 3363 (OH) and 1633 cm^{-1} (C=C−C=O). The ^1H NMR spectrum revealed the presence of a *para*-disubstituded benzene ring characterized by signals at δ 7.52 (2H, d, J = 8.5 Hz) and 6.88 (2H, d, J = 8.5 Hz); a 1,3,4-trisubstituted benzene ring [δ 6.85 (H-2″, d, J = 2.0 Hz), 6.72 (H-5″, d, J = 8.4 Hz), and 6.68 (H-6″, dd, J = 8.4, 2.0 Hz)]; a pair of *trans* olefinic protons at δ 7.53 (H-7, d, J = 15.9 Hz) and 6.53 (H-6, d, J = 15.9 Hz); a methoxy signal at δ 3.80 (s); and two methylenes at δ 2.85 and 2.67 (each triplet, J = 8.1 Hz). This was in sound agreement with the ^{13}C NMR spectrum (Table 1), which showed signals attributed to a carbonyl at δ 199.9 (C-3) and a hydroxylated olefinic carbon at δ 178.5, which with subsequent HMBC cross correlation peak with the *trans* olefinic protons as well as with H-4 (δ 5.81) was attributed to C-5. Three oxygenated sp^2 carbon atoms were also observed at δ 145.9, 148.3, and 160.5. A judicious analysis of the $^1H-^1H$ COSY data of **1** implied connectivities of H-7 to H-6, H-2 to H-1, H-2′ to H-3′ and H-6′, H-5′ to H-3′ and H-6′, and H-6″ to H-2″ and H-5″. The correlations observed in the NOESY and HMBC spectra attached the methoxy group at position C-3″ rather than C-4″, and pertinent correlation peaks were observed between the OMe group (δ 3.80) and H-2″ (δ 6.85) in the NOESY spectrum and between the OMe protons and C-3″ in the HMBC spectrum. The stereochemistry of the C-6/C-7 double bond bond is *E* as judged by the coupling constant between the two protons (J = 15.9 Hz), and that of the C-4 double bond is *Z*, as a clear NOESY correlation peak was observed between H-4 and H-6. Further analysis of HMBC and NOESY spectra led to the assignment of all carbons and protons, and the structure of compound **1** is (4*Z*,6*E*)-5-hydroxy-1-(4-hydroxy-3-methoxyphenyl)-7-(4-hydroxyphenyl)hepta-4,6-dien-3-one. The trivial name letestuianin A was given to this new diarylheptanoid.

Compound **2** was obtained as yellow needles (CH_2Cl_2), mp 179−180 °C. The EIMS of **2** showed a molecular ion peak at *m*/*z* 370 compatible with the molecular formula $C_{21}H_{22}O_6$. The IR spectrum showed absorption bands due

* To whom correspondence should be addressed. Tel: (46) 46 222 8213. Fax: (46) 222 8209. E-mail: Olov.Sterner@bioorganic.lth.se (O.S). Tel: (1) 212 346 1246. Fax: (1) 212 346 1586. E-mail: cbacchi@fsmail.pace.edu (C.B).
[†] University of Dschang.
[||] Deceased.
[‡] Lund University.
[§] Pace University.
[⊥] Walter Reed Army Institute of Research.

10.1021/np020362f CCC: $25.00
Published on Web 02/19/2003

Table 1. ^{13}C (125 MHz) and ^{1}H NMR (500 MHz) Data for Compounds **1**, **2**, and **3**

	1[a]		**2**[b]		**3**[c] (major component)	
position	^{13}C	^{1}H	^{13}C	^{1}H	^{13}C	^{1}H
1	31.7	2.85 t (8.1)	30.4	2.77 t (8.0)	29.7	2.71 s
2	42.7	2.67 t (8.1)	41.3	2.65 t (8.0)	46.4	2.71 s
3	199.5		199.2		206.5	
4	101.0	5.81 s	100.2	5.90 s	57.4	3.52 s
5	178.5		177.9		206.5	
6	120.8	6.53 d (15.9)	119.7	6.63 d (15.9)	46.4	2.71 s
7	140.6	7.53 d (15.9)	140.2	7.45 d (15.9)	29.7	2.71 s
1′	127.8		126.3		133.0	
2′	130.9	7.52 d (8.5)	111.0	7.25 d (2.0)	130.4	6.98 d (8.5)
3′	116.9	6.88 d (8.5)	148.0		116.3	6.68 d (8.5)
4′	160.5		149.2		156.7	
5′	116.9	6.88 d (8.5)	115.7	6.78 d (8.0)	116.3	6.68 d (8.5)
6′	130.9	7.52 d (8.5)	123.0	7.13 dd (8.0, 2.0)	130.4	6.98 d (8.5)
1″	133.4		131.6		133.0	
2″	112.9	6.85 d (2.0)	112.5	6.77 d (2.0)	130.4	6.98 d (8.5)
3″	148.3		147.4		116.3	6.68 d (8.5)
4″	145.9		144.7		156.7	
5″	115.8	6.72 d (8.4)	115.3	6.64 d (7.9)	116.3	6.68 d (8.5)
6″	121.6	6.68 dd (8.4, 2.0)	120.3	6.59 dd (7.9, 2.0)	130.4	6.98 d (8.5)
OMe′			55.7	3.78 s		
OMe″	56.3	3.80 s	55.5	3.71 s		

[a] Spectra recorded in acetone-d_6. [b] Spectra recorded in DMSO-d_6. [c] Spectra recorded in CD_3OD.

to hydroxyl group(s), enone, and aromatic ring(s) functionalities at ν_{max} 3436, 1631, and 1602 cm^{-1}, respectively. The ^{1}H and ^{13}C NMR data (Table 1) of **2** were closely related to those of compound **1**. The only significant differences compared to **1** are that both aromatic systems are 1,3,4-trisubstituted and the presence of an additional methoxy group in **2**. Once more the NOESY spectrum was useful for the determination of the position of the methoxy groups on the aromatic rings as well as for the *Z* conformation of one of the double bond. Important correlation peaks were observed between the OMe at δ 3.71 and the proton at δ 6.77 (d, $J = 2.0$ Hz) as well as the OMe at δ 3.78 and the proton at δ 7.25 (d, $J = 2.0$ Hz). Together with COSY and HMBC data the structure (4*Z*,6*E*)-5-hydroxy-1,7-bis(4-hydroxy-3-methoxyphenyl)hepta-4,6-dien-3-one was determined for compound **2**, and it was given the trivial name letestuianin B.

Compound **3** was obtained as a pale yellow oil. The EIMS spectrum of **3** showed a molecular ion peak at *m/z* 312 compatible with the molecular formula $C_{19}H_{20}O_4$. The IR spectrum showed absorption bands at ν_{max} 3407, 1630, 1613, 1515, and 828 cm^{-1} closely related to those of **1** and **2**. The 1D NMR spectra suggested the presence of two components, in a 3:7 ratio. For the major component, the ^{1}H NMR spectrum indicated the presence of a *para*-disubstituted benzene ring [δ 6.98 (2H, d, $J = 8.5$ Hz) and 6.68 (2H, d, $J = 8.5$ Hz)] and two methylenes appearing as singlet at δ 2.71. An isolated proton appeared at δ 3.52 as a singlet. The intensity of the latter signal was very low due to exchange with deuterium from the methanol solvent used for NMR experiments. These data account only for nine protons, and the fact that only eight carbon signals appeared in its ^{13}C NMR spectrum suggests that **3** is symmetric with two identical benzene rings. The data for the major component were compatible only with the 1,3-diketone shown in Figure 1, and as expected, this is in equilibrium with an enol tautomer. Typical signals for the enol appeared in the ^{1}H and ^{13}C NMR spectra, for example a proton signal at δ 4.58 (H-4) and carbon signals at δ 194.7 (C-3) and 100.0 (C-4), but to confirm this tautomeric equilibrium, compound **3** was treated with a mixture of pyridine−Ac_2O (1:1) to give the acetylated derivative **4**. The analysis of the ^{1}H NMR spectrum of **4** revealed the presence of a 1,4-disubstituted benzene ring, showing that

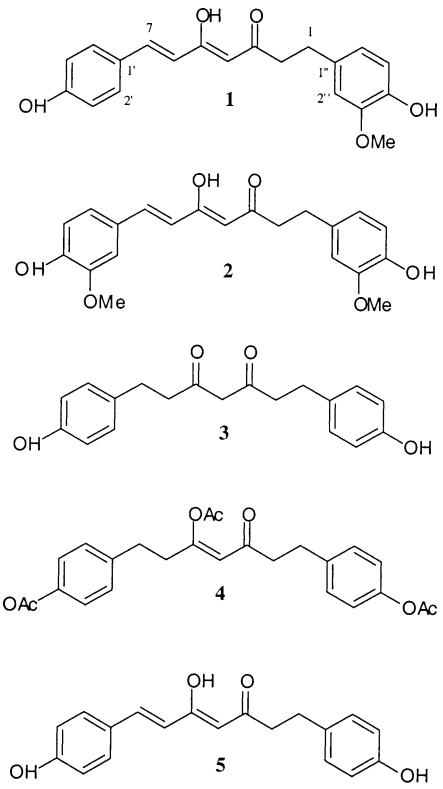

Figure 1.

the symmetric nature of the molecule had been distorted. An olefinic signal was also observed in **4** at δ 5.42 in replacement of the methylene signal that was present at δ 3.52 in **3**. The presence of three acetate functions was characterized by shifts at δ 2.22 (6H, s) and 2.10 (3H, s). The analysis of the ^{13}C NMR spectrum of **4** with signals at δ 169.5, 169.7, and 170.0 confirmed the three acetate functions. A conjugated carbonyl function was also observed at δ 193.2. All the above information showed that **4** was the enol form of **3**. Further analysis of HMBC, COSY, and NOESY spectra of the nonacetylated and acetylated derivative led to the characterization of compound **3** as 1,7-bis(4-hydroxyphenyl)heptan-3,5-dione, consequently named letestuianin C.

Table 2. Antitrypanocidal Activities of *Aframomum letestuianum* Diarylheptanoids

	IC_{50} (μg/mL)		
		KETRI *T. b. rhodesiense* KETRI isolates	
compound	Lab110 EATRO *T. b. brucei*	243	243 As 10−3
1	>100		
2	67	>100	>100
3	1.4	2.3	2.6
5	2.6	2.8	1.3
melarsoprol	0.002	0.0005	0.005
pentamidine	0.0006	0.0005	0.004

Previous studies on the genus *Aframomum* have, up to date, reported the presence of only two major classes of natural products, diterpenoids and flavonoids. To the best of our knowledge, **1**, **2**, **3**, and **5** are the first diarylheptanoids reported from this important genus, although they are common in the sister genera *Alpinia*[9−11] and *Curcuma*.[12−14] The four diarylheptanoids obtained were assayed for trypanocidal activity, tested against bloodstream forms of *Trypanosoma b. brucei* and *Trypanosoma b. rhodesiense* isolates grown in vitro in 24-well plates. Coulter counts were made daily, and the IC_{50} values determined after 48 h are given in Table 2. Compound **1** was not growth inhibitory below 100 μg/mL. Compound **2** gave an IC_{50} value of 67 μg/mL with the *T. b. brucei* isolate but >100 μg/mL with *T. b. rhodesiense* isolates. Compounds **3** and **5**, however, were highly effective in the range 1−3 μg/mL for all isolates tested. Interestingly, the additional methoxy group in **1**, compared to **5**, makes it inactive. Corresponding IC_{50} values for the trypanocides melarsoprol and pentamidine were ~300−5000-fold lower; however, lack of sufficient material prevented us from testing these compounds in vivo in a mouse model infection.

Experimental Section

General Experimental Procedures. Melting points were recorded with a Reichter microscope and are uncorrected. The UV and IR spectra (KBr) were recorded with a Shimadzu UV-3001 and a Jasco FT-IR spectrophotometer, respectively. ^{1}H NMR and ^{13}C NMR were recorded in $CDCl_3$, acetone-d_6, DMSO-d_6, or CD_3OD using a Bruker ARX500 spectrometer with an inverse multinuclear 5 mm probe head equipped with a shielded gradient coil. The chemical shifts (δ) are reported in parts per million relative to tetramethylsilane (TMS, δ = 0), while the coupling constants (J) are given in Hz. COSY, HMQC, and HMBC experiments were recorded with gradient enhancements using sine-shaped gradient pulses. For 2D heteronuclear correlation spectroscopy the refocusing delays were optimized for $^1J_{CH}$ = 145 Hz and $^nJ_{CH}$ = 10 Hz. The raw data were transformed and the spectra evaluated with the standard Bruker UXNMR software. The positive EI (70 eV) and CI mass spectra were recorded with a JEOL SX102 spectrometer. Column chromatography was run on Merck Si gel 60 and gel permeation on Sephadex LH-20. TLC analyses were carried out on Si gel GF_{254} precoated plates with detection accomplished by spraying with 50% H_2SO_4 followed by heating at 100 °C, or by visualizing with a UV lamp at 254 and 366 nm.

Plant Material. The seeds of *A. letestuianum* were collected from Abong-bang, East Province, Cameroon, in December 1998. Mr. Paul Mezili, a retired botanist of the Cameroon Herbarium, authenticated the plant material. Voucher specimens (BUD 0391) were deposited at the Herbarium of the Botany Department of the University of Dschang.

Extraction and Isolation. The air-dried powdered seeds of *A. letestuianum* (2 kg) were macerated with a mixture (1:1) of MeOH−CH_2Cl_2 (4 L) overnight and evaporated in vacuo to yield a crude extract (150.5 g). This crude extract was dissolved in 80% MeOH (600 mL) and extracted hexane (3 × 500 mL). The aqueous MeOH was further diluted with water to 60%MeOH and extracted with CH_2Cl_2 (3 × 500 mL). Vacuum concentration yielded CH_2Cl_2 extract (36.5 g) and hexane extract (28.0 g), which contained mostly fats. Subjection of the CH_2Cl_2 extract to column chromatography over silica gel eluting with a CH_2Cl_2−hexane gradient followed by acetone−CH_2Cl_2 afforded three major fractions, I [500 mg, CH_2Cl_2−hexane (6:4)], II [16.0 g, CH_2Cl_2−hexane (8:2) and acetone−CH_2Cl_2 (1:9)], and III [2.1 g, acetone−CH_2CL_2 (2:8)]. Subjecting fraction I to repeated column chromatography on silica gel eluted with a CH_2Cl_2−hexane gradient and further purification by gel permeation chromatography on Sephadex LH-20 (MeOH) afforded compounds **1** (24 mg), **2** (10.4 mg), and 7-methoxy-3,5,4′-trihydroxyflavanone (5.5 mg). Subjection of fraction II (7.5 g) to gel permeation chromatography on Sephadex LH-20 (MeOH) gave additional amount of **1** (15 mg), 3-acetoxy-5,7,4′-trihydroxyflavanone (3.5 g), 3-acetoxy-7-methoxy-5,4′-dihydroxyflavanone (1.8 g), and a mixture of two main products (350 mg), which was further purified by countercurrent chromatography (CCC) eluting head to tail with hexane−ethyl acetate−MeOH−H_2O (4:6:5:5) and reversing the flow after 3 h to obtain compounds **3** (179 mg) and **5** (86 mg). Treatment of fraction III on a silica gel column eluted with MeOH−CH_2Cl_2 gradient followed by gel permeation on Sephadex LH-20 (MeOH−CH_2Cl_2, 1:1) afforded 3,3′,4′,5,7-pentahydroxyflavan (139 mg) and a mixture of nonresolved compounds.

(4*Z*,6*E*)-5-Hydroxy-1-(4-hydroxy-3-methoxyphenyl)-7-(4-hydroxyphenyl)hepta-4,6-dien-3-one, letestuianin A (1): yellowish oil; UV (MeOH) λ_{max} (log ϵ) 380 (3.2) and 283 (3.9) nm; IR (KBr) ν_{max} 3363, 2937, 1633, 1583, 1514, 1431, 831, and 790 cm^{-1}; ^{1}H and ^{13}C NMR data, see Table 1; EIMS *m*/*z* 340 [M]$^+$ (100), 322 (10), 189 (30), 147 (70), 137 (55), 107 (18); HREIMS *m*/*z* 340.1304 (calcd for $C_{20}H_{20}O_5$, 340.1311).

(4*Z*,6*E*)-5-Hydroxy-1,7-bis(4-hydroxy-3-methoxyphenyl)-hepta-4,6-dien-3-one, letestuianin B (2): shiny yellow needles (CH_2Cl_2−hexane); mp 179−180 °C; UV (MeOH) λ_{max} (log ϵ) 374 (2.9) and 288 (3.4) nm; IR (KBr) ν_{max} 3436, 1631, 1602, 1511, 1280, 1202, 1028, and 814 cm^{-1}; ^{1}H and ^{13}C NMR data, see Table 1; EIMS *m*/*z* 370 [M]$^+$ (44), 352 (16), 219 (18), 177 (63), 137 (100), 44 (25); HREIMS *m*/*z* 370.1411 (calcd for $C_{21}H_{22}O_6$, 370.1416).

1,7-Bis(4-hydroxyphenyl)heptan-3,5-dione, letestuianin C (3): yellowish oil; UV (MeOH) λ_{max} (log ϵ) 279 (3.4) and 224 (2.4) nm; IR (KBr) ν_{max} 3407, 1623, 1613, 1515, 1462, 1385, 1243, 828 cm^{-1}; ^{1}H and ^{13}C NMR data, see Table 1; EIMS *m*/*z* 312 [M]$^+$ (34), 191 (10), 120 (20), 107 (100), 77 (10); HREIMS *m*/*z* 312.1358 (calcd for $C_{19}H_{20}O_4$, 312.1361).

Acetylation of Letestuianin C (3). Compound **3** (25 mg) was dissolved in a (1:1) mixture of pyridine−Ac_2O (4 mL) and the reaction mixture left at room temperature overnight. The product was concentrated with addition of toluene and purified on a silica gel column (hexane−EtOAc, 9:1) to give 5-acetoxy-1,7-bis(4-acetoxyphenyl)hepta-4-en-3-one (**4**) (26 mg) as a colorless oil: ^{1}H NMR ($CDCl_3$, 500 MHz) δ 2.10 (Ac), 2.22 (2 × Ac), 2.52 (4H, t, J = 7.6 Hz, H-2, H-6), 2.81 (4H, t, J = 7.6 Hz, H-1, H-7), 5.42 (H-4, s), 6.90 (4H, m, H-2′, H-6′, H-2″, H-6″), 7.23 (4H, m, H-3′, H-5′, H-3″, H-5″); ^{13}C NMR $CDCl_3$, 125 MHz) δ 31.2 (C-1, C-7), 40.3 (C-2, C-6), 100.1 (C-4), 121.9 (C-3″, C-5″), 122.0 (C-3′, C-5′) 129.7 (C-2″, C-6″), 129.8 (C-2′, C-6′), 138.5 (C-1″), 138.6 (C-1′), 149.4 (C-4′, C-4″), 179.1 (C-5), 193.2 (C-3).

Biological Assay. Assays for inhibition of trypanosomal growth were conducted as previously described.[15,16] Bloodstream-form trypanosomes were cultured in modified IMDM with 20% horse serum at 37 °C. Drug studies were done in duplicate in 24-well plates (1 mL/well) with final inhibitor concentrations of 0.1, 1, 10, 25, and 100 μg/mL. Wells were inoculated with 10^5 trypanosomes, and one-half the volume of each well was changed daily. After 48 h, the parasite number was determined in a Model Z1 Coulter counter and IC_{50} values were calculated from semi-log plots. Assays were done two or more times, using widely spaced concentration curves initially, followed by curves of closely spaced values to obtain the IC_{50} value.

Compounds were dissolved in 100% dimethyl sulfoxide and diluted in medium, so that the dimethyl sulfoxide concentration never exceeded 0.3%, a noninhibitory concentration.

Strains used were *Trypanosoma b. brucei* Lab 110 EATRO and Kenya Trypanosomiasis Research Institute (KETRI) isolates *Trypanosoma b. rhodesiense* 243 and 243 As 10-3.[15,16]

Acknowledgment. The authors gratefully acknowledge financial support from the Fogarty International Center (NIH Grant 1U01TWO 0317, as part of the International Cooperative Biodiversity Group Program) and the Swedish Natural Science Research Council.

References and Notes

(1) Koechlin, J. F. *Flore du Cameroun*: *Scitaminales*; Muséum National de l'Histoire Naturelle: Paris, 1965; p 4.
(2) Thomas, D. W.; Thomas, J.; Bromley, W. N.; Mbenkum, F. T. *Korup Ethnobotany Survey, Final Report to: The World Wide Fund for Nature*; Penda House: Weyside Park, Godalming: Surrey, U.K.; 1989.
(3) Ayafor, J. F.; Tchuendem, M. K. H.; Nyasse, B.; Tillequin, F.; Anke, H. *Pure Appl. Chem*. **1994**, *66*, 2327−2330.
(4) Ayafor, J. F.; Connolly, J. D. *J. Chem. Soc., Perkin Trans. 1* **1981**, 2563−2565.
(5) Tsopmo, A.; Tcheundem, M. K. H.; Ayafor, J. F.; Tillequin, F.; Kock, M.; Anke, H. *Nat. Prod. Lett*. **1996**, *9*, 93.
(6) Tchuendem, M. H. K.; Mbah, J. A.; Tsopmo, A.; Ayafor, J. F.; Okunji, C.; Iwu, M. M.; Schuster, B. M. *Phytochemistry* **1999**, *52*, 1095−1099.
(7) Hui, D.; Sao-Xing, C. *J. Nat. Prod*. **1998**, *61*, 142−144.
(8) Aldrich Libray of ^{13}C and ^{1}H FT NMR spectra **1992**, *2*, 326A.
(9) Kadota, S.; Hui, D.; Basnet, P.; Prasain, J. K.; Xu, G.; Namba, T. *Chem. Pharm. Bull*. **1994**, *42*, 2647−2649.
(10) Itokawa, H.; Morita, M.; Midorikawa, I.; Aiyama, R.; Morita, M. *Chem. Pharm. Bull*. **1985**, *33*, 4889−4893.
(11) Kiuchi, F.; Shibuya, M.; Sankawa, U. *Chem. Pharm. Bull*. **1982**, *30*, 2279−2282.
(12) Kiuchi, F.; Goto, Y.; Sugimoto, N.; Akao, N.; Kando, K.; Tsuda, Y. *Chem. Pharm. Bull*. **1992**, *41*, 1640−1643.
(13) Masuda, T.; Jitoe, A.; Nakatani, N.; Yonemori, S. *Phytochemistry* **1993**, *33*, 1557−1560.
(14) Uehara, S.; Yasuda, I.; Akiyama, K.; Morita, H.; Takeya, K.; Itokawa, H. *Chem. Pharm. Bull*. **1978**, *35*, 3298−3304.
(15) Hirumi, H.; Hirumi, L. *J. Parasitol*. **1989**, *75*, 985−989.
(16) Sufrin, J. R.; Rattendi, D.; Spiess, A. J.; Lane, S.; Marasco, C. J., Jr.; Bacchi, C. J. *Antimicrob. Agents Chemother*. **1996**, *40*, 2567−2572.

NP020362F